

Molecular P_ψ pentaquarks from light-meson exchange saturation

Zi-Ying Yang,¹ Fang-Zheng Peng,^{2,3} Mao-Jun Yan,^{4,5} Mario Sánchez Sánchez,^{6,7} and Manuel Pavon Valderrama^{1,*}

¹*School of Physics, Beihang University, Beijing 100191, China*

²*Southern Center for Nuclear-Science Theory (SCNT), Institute of Modern Physics, Chinese Academy of Sciences, Huizhou 516000, China*

³*Institute of Modern Physics, Chinese Academy of Sciences, Lanzhou 730000, China*

⁴*CAS Key Laboratory of Theoretical Physics, Institute of Theoretical Physics, Chinese Academy of Sciences, Beijing 100190*

⁵*School of Physical Science and Technology, Southwest University, Chongqing 400715, China*

⁶*LP2IB (CNRS/IN2P3 – Université de Bordeaux), 33175 Gradignan cedex, France*

⁷*Departamento de Física, Universidad de Murcia, 30071 Murcia, Spain*

(Dated: January 17, 2025)

Theoretical predictions of the spectrum of heavy meson-baryon bound states are a fundamental tool for disentangling the nature of the different pentaquark states that have been observed in experimental facilities. Here we explore this spectrum in a phenomenological model that describes the heavy meson-baryon interaction in terms of a contact-range interaction, where the coupling strength is saturated by the exchange of light scalar and vector mesons, i.e. σ , ρ and ω exchanges. Saturation determines the couplings modulo an unknown proportionality constant that can be calibrated from a molecular candidate. If we use the $P_\psi^N(4312)$ as input, we predict a series of molecular pentaquarks including the $P_\psi^N(4440)$ and $P_\psi^N(4457)$, the recent $P_{\psi_s}^\Lambda(4338)$ and the $P_{\psi_s}^\Lambda(4459)$.

I. INTRODUCTION

Recently the LHCb collaboration has observed [1] a new pentaquark state within the $J/\psi\Lambda$ invariant mass distribution. Its mass and width (in units of MeV) are

$$M = 4338.2 \pm 0.7, \quad \Gamma = 7.0 \pm 1.2, \quad (1)$$

and its spin-parity is $J^P = \frac{1}{2}^-$. This $P_{\psi_s}^\Lambda(4338)$ pentaquark is simply the latest addition to a growing family of hidden-charm pentaquark states, which includes the $P_{\psi_s}^\Lambda(4459)$ [2], also discovered in $J/\psi\Lambda$ and with mass and width (MeV)

$$M = 4458.8 \pm 2.9_{-1.1}^{+4.7}, \quad \Gamma = 17.3 \pm 6.5_{-5.7}^{+8.0}, \quad (2)$$

or the three P_ψ^N states discovered in 2019 [3] — the $P_\psi^N(4312)$, $P_\psi^N(4440)$ and $P_\psi^N(4457)$ — whose masses and widths are, respectively (again in MeV):

$$M = 4311.9 \pm 0.7_{-0.6}^{+6.8}, \quad \Gamma = 9.8 \pm 2.7_{-4.5}^{+3.7}, \quad (3)$$

$$M = 4440.3 \pm 1.3_{-4.7}^{+4.1}, \quad \Gamma = 20.6 \pm 4.9_{-10.1}^{+8.7}, \quad (4)$$

$$M = 4457.3 \pm 0.6_{-1.7}^{+4.1}, \quad \Gamma = 6.4 \pm 2.0_{-1.9}^{+5.7}. \quad (5)$$

The masses of the aforementioned pentaquarks are all close to charmed antimeson - charmed baryon thresholds and have thus been theorized to be molecular, where specific discussions can be found in [4–8] for the $P_{\psi_s}^\Lambda(4338)$, in [9–12] for the $P_{\psi_s}^\Lambda(4459)$ and in [13–20] for the $P_\psi^N(4312/4440/4457)$. Yet, there are also non-molecular explanations [21–26] and at least one pentaquark — the $P_\psi^N(4337)$ [27] — that is more difficult to accommodate within the molecular picture [28, 29].

Here we will consider the previous five pentaquarks from a molecular perspective¹. We are interested in the question of

whether they can be explained with the same set of parameters in the phenomenological model we proposed in [30]. This model describes molecular states in terms of a simple contact-range interaction in which the exchange of light-mesons — the scalar σ and the vector ρ and ω mesons — saturates the couplings. The rationale behind the choice of a contact-range theory is that the size of most hadronic bound states is not small enough to probe the details of the light-meson exchange potential, hence the simplification of the interaction from finite- to contact-range. A few of these pentaquarks have indeed been explained (or even predicted [31–33]) by the exchange of light-mesons [34–36]. Yet, these models usually (though not always [36]) concentrate on a particular sector (non-strange/strange). By treating the non-strange and strange sectors on the same footing, we will be able to answer the question of whether the P_ψ^N and $P_{\psi_s}^\Lambda$ pentaquarks are indeed connected.

II. SATURATION OF THE CONTACT-RANGE COUPLINGS

In the molecular picture the hidden-charmed pentaquarks are charmed antimeson - charmed baryon two-body systems. We describe the antimeson-baryon interaction in terms of a non-relativistic S-wave contact-range potential of the form

$$\langle \vec{p}' | V_C | \vec{p} \rangle = C_0 + C_1 \hat{S}_{L1} \cdot \hat{S}_{L2}, \quad (6)$$

where there is a central and spin-spin piece, with C_0 and C_1 their respective couplings, and with $\hat{S}_{Li} = \vec{S}_{Li}/|S_{Li}|$ the normalized light-quark spin operator of hadron $i = 1, 2$ (with $i = 1$ the antimeson and $i = 2$ the baryon). Being a contact-range interaction, this potential has to be regularized, which we will do by introducing a regularization scale Λ , i.e. a cut-off. Details on the specific regularization procedure will be given later on.

* mpavon@buaa.edu.cn

¹ By *molecular* we specifically refer to composite in the sense that most of the wave function of the state corresponds to a meson-baryon component (instead of a multi-quark component).

This description is expected to be a good approximation to the baryon-antimeson potential provided the two following conditions are met: (i) the binding momentum of the molecular pentaquarks is smaller than the mass of the light-mesons generating the binding, which we suspect to be the scalar and vector mesons, and (ii) that long-range effects, such as one pion exchange (OPE) are perturbative. The first of these conditions is met for the molecular interpretations of the $P_\psi^N(4312/4440/4457)$ and $P_{\psi s}^\Lambda(4338/4459)$ pentaquarks, i.e. $\bar{D}^{(*)}\Sigma_c$ and $\bar{D}^{(*)}\Xi_c$ bound states. Indeed, the binding momentum of these systems (defined as $\gamma = \sqrt{2\mu B}$ with μ the reduced mass of the two-body system and B the binding energy) is of the order of $(100 - 200)$ MeV, while the ρ meson mass is about 770 MeV. The second of these conditions is trivially met for the $\bar{D}\Sigma_c$ and $\bar{D}^{(*)}\Xi_c$ systems, for which OPE is forbidden, while for the $\bar{D}^*\Sigma_c$ case there are EFT arguments [17] and explicit calculations in the phenomenological model we are using here [30] that show that OPE is indeed a perturbative correction and can be safely neglected in a first approximation.

The couplings C_0 and C_1 are assumed to be saturated by scalar and vector meson exchange. We first remind that the potentials generated by the scalar and vector light-mesons are

$$V_S = -\frac{g_{S1}g_{S2}}{m_S^2 + \vec{q}^2}, \quad (7)$$

$$V_V = (\zeta + T_{12}) \left[\frac{g_{V1}g_{V2}}{m_V^2 + \vec{q}^2} + \frac{f_{V1}f_{V2}}{6M^2} \frac{m_V^2}{m_V^2 + \vec{q}^2} \hat{S}_{L1} \cdot \hat{S}_{L2} \right] + \dots, \quad (8)$$

where m_S and m_V are the scalar and vector meson masses, g_{Si} , g_{Vi} , and f_{Vi} are coupling constants (with $i = 1, 2$ indicating whether we are referring to the charmed antimeson or baryon), M a scaling mass, which we take to be $M = m_N$ with $m_N = 938.9$ MeV the nucleon mass, and the dots represent either Dirac-deltas or higher partial wave contributions to the potential. The vector meson potential has been written for the particular case in which only the ρ and ω mesons are exchanged, i.e. for the $\bar{D}^{(*)}\Sigma_c^{(*)}$ and $\bar{D}^{(*)}\Xi_c^{(*)}$ systems, where $\zeta = \pm 1$ is the sign of ω exchange ($\zeta = +1$ for hidden-charm pentaquarks and $\zeta = -1$ for doubly charmed ones) and T_{12} is an isospin factor given by $T_{12} = \vec{\tau}_1 \cdot \vec{\tau}_2$ for $\bar{D}^{(*)}\Sigma_c^{(*)}$ and $T_{12} = \vec{\tau}_1 \cdot \vec{\tau}_2$ for $\bar{D}^{(*)}\Xi_c^{(*)}$, where we remind that $\vec{\tau}_i$ (\vec{T}_i) are the Pauli (spin-1) matrices when acting on the isospin degrees of freedom of an isospin-1/2 (isospin-1) hadron. For the masses of the light mesons we take $m_S = 475$ MeV (i.e. the average of its $(400 - 550)$ MeV mass range in the Review of Particle Physics (RPP) [37]) and $m_V = (m_\rho + m_\omega)/2 = 775$ MeV (i.e. the average of the ρ and ω masses). For the scalar meson couplings, we use the linear sigma model [38] and the quark model [39] plus the assumption that the coupling of the scalar meson to the u , d and s quarks is the same, yielding $g_S = 3.4$ and 6.8 for the charmed mesons and baryons, respectively. For the vector meson couplings we use Sakurai's universality and vector meson dominance [40–42] to obtain $g_V = 2.9$ and 5.8 for the charmed mesons and $\Sigma_c^{(*)}$ baryons and $g_V = 2.9$ for the $\Xi_c^{(*)}$ baryons; for the magnetic-like couplings we define

$f_V = \kappa_V g_V$ with $\kappa_V = \frac{3}{2} (\mu_u/\mu_N)$ for both charmed mesons and sextet charmed baryons (Σ_c , Σ_c^* , Ξ_c' , Ξ_c^*), with μ_N the nuclear magneton and $\mu_u \simeq 1.9 \mu_N$ the magnetic moment of a constituent u-quark. In contrast, for antitriplet charmed baryons (Ξ_c) we have $\kappa_V = 0$ instead. The extension to the other molecular configurations can be done by modifying the vector meson masses to take into account that the K^* and ϕ vector mesons are heavier than the ρ and ω and by changing the $(\zeta + T_{12})$ factor by the corresponding SU(3)-flavor factor (we will explain these changes in more detail later on).

Provided we use a regularization scale of the same order of magnitude as the mass of the light mesons, the saturation of the couplings by a scalar meson will be given by

$$C_0^S(\Lambda \sim m_S) \propto -\frac{g_{S1}g_{S2}}{m_S^2}, \quad (9)$$

$$C_1^S(\Lambda \sim m_S) \propto 0, \quad (10)$$

while the saturation by a vector meson will be

$$C_0^V(\Lambda \sim m_V) \propto \frac{g_{V1}g_{V2}}{m_V^2} (\zeta + T_{12}), \quad (11)$$

$$C_1^V(\Lambda \sim m_V) \propto \frac{f_{V1}f_{V2}}{6M^2} (\zeta + T_{12}), \quad (12)$$

where the proportionality constant is, in principle unknown, and must be determined from external information. In the particular case of vector meson exchange we have followed the novel saturation method proposed in [43].

Owing to $m_S \neq m_V$, it is apparent that the ideal regularization scale for the saturation of the C_0 coupling by the scalar and vector mesons is not identical. This is dealt with by considering the renormalization group evolution (RGE) of the contact-range potential V_C , which is given by [44]

$$\frac{d}{d\Lambda} \langle \Psi | V_C(\Lambda) | \Psi \rangle = 0, \quad (13)$$

where Ψ represents the wave function of the two-body bound state under consideration and Λ the regularization scale. If the r-space wave function displays a power-law behavior of the type $\Psi(r) \sim r^{\alpha/2}$ at distances $r \sim 1/\Lambda$, the previous RGE becomes

$$\frac{d}{d\Lambda} \left[\frac{C(\Lambda)}{\Lambda^\alpha} \right] = 0, \quad (14)$$

where $C(\Lambda) = C_0(\Lambda) + C_1(\Lambda) \hat{S}_{L1} \cdot \hat{S}_{L2}$. This implies the following relation of the couplings when evaluated at different regularization scales:

$$\frac{C(\Lambda_1)}{\Lambda_1^\alpha} = \frac{C(\Lambda_2)}{\Lambda_2^\alpha}. \quad (15)$$

That is, provided α is known, it will be trivial to combine the contributions from scalar and vector meson exchange to the saturation of the couplings. In particular, if we fix the

regularization scale to the vector meson mass, we will have

$$C(\Lambda = m_V) = C_V(m_V) + \left(\frac{m_V}{m_S}\right)^\alpha C_S(m_S) \\ \propto \frac{g_{V1}g_{V2}}{m_V^2} [\zeta + T_{12}] \left(1 + \kappa_{V1\kappa_{V2}} \frac{m_V^2}{6M^2} \hat{C}_{L12}\right) \\ - \left(\frac{m_V}{m_S}\right)^\alpha \frac{g_{S1}g_{S2}}{m_S^2}, \quad (16)$$

where $\hat{C}_{L12} = \hat{S}_{L1} \cdot \hat{S}_{L2}$.

The only problem is determining the scaling power α . From the regularity of the wave function at the origin, we expect $\Psi(r) \sim 1$ for $r \rightarrow 0$, yielding $\alpha = 0$. But this is only the case for point-like particles: the finite size of hadrons will suppress the two-body wave functions at distances of the order of the hadron size (i.e. the molecular probability decreases, while the probability that the state is in a multi-quark configuration increases). This observation implies that $\alpha > 0$. For instance, if we include a Lorentzian form factor in the momentum space representation of the wave function, i.e. a factor of the type $1/(1 + (q/M)^2) \rightarrow M^2/q^2$ for $q \gg M$ with M the momentum scale at which the structure of hadrons becomes evident, this translates into an $(Mr)^2$ suppression at distances $(Mr) \ll 1$, suggesting $\alpha = 2$. Yet, scalar and vector meson exchange still involve slightly lower momenta than the ones for which the internal structure of the hadrons becomes evident ($M \sim 1$ GeV). Thus we will choose $\alpha = 1$, which takes into account that meson-exchanges happen in a region where the internal structure of hadrons is not fully resolved, yet considering them as point-like is not a good approximation either².

It is worth noticing that though we have expressed $C(\Lambda)$ for $\Lambda = m_V$, it is perfectly acceptable to vary Λ around this value: from Eqs. (14,15) we see that changing the regularization scale will simply change the proportionality constant in the second line of Eq. (16). Yet, we remind that we are dealing with a phenomenological model (and not with an effective field theory): ultimately the value of Λ is a parameter of the model and the criterion by which it is chosen is the reproduction of known features of the pentaquark spectrum (an observation which is also applicable to the parameter α we discussed in the previous paragraph).

III. CALIBRATION AND PREDICTIONS

A. Basic formalism

For predictions to be made in this model, we first have to determine the unknown proportionality constant in Eq. (16).

² A more practical reason is that with $\alpha = 1$ the results of the RG-improved saturation method presented are basically the same as the ones obtained with the one-boson-exchange model for the molecular $\Sigma_c^{(*)}\bar{D}^{(*)}$ pentaquarks when both methods are calibrated to reproduce the mass of the $P_\psi^N(4312)$ state [18].

This is done by choosing a *reference state* — a state that is assumed to be a particular type of two-body bound state — and then calculating the strength of the coupling constant for this state. Our choice of a reference state will be the $P_\psi^N(4312)$ pentaquark as a $\Sigma_c\bar{D}$ bound state.

The way this is done is straightforward, though it involves a few steps. First, we begin by regularizing the contact-range potential with a specific separable regulator function $f(x)$

$$V_C = C_{\text{mol}}^{\text{sat}}(\Lambda) f\left(\frac{P'}{\Lambda}\right) f\left(\frac{P}{\Lambda}\right), \quad (17)$$

for which we will choose a Gaussian, $f(x) = e^{-x^2}$ and where $C_{\text{mol}}^{\text{sat}}$ is the saturated coupling for a particular molecular state “mol”. The regularization scale will be taken to be $\Lambda = 1.0$ GeV, i.e. the value we already used in [30]. The regularized potential is then inserted in the Lippmann-Schwinger equation for the bound state pole, which for a separable interaction takes the simplified form

$$1 + C_{\text{mol}}^{\text{sat}}(\Lambda) \int \frac{d^3\vec{q}}{(2\pi)^3} \frac{f^2\left(\frac{q}{\Lambda}\right)}{M_{\text{th}} + \frac{q^2}{2\mu_{\text{mol}}} - M_{\text{mol}}} = 0, \quad (18)$$

which implicitly assumes that we are dealing with a single-channel problem. Here M_{mol} refers to the mass of the molecule (or pole of the T-matrix), $M_{\text{th}} = m_1 + m_2$ to the mass of the two-body threshold and $\mu = m_1 m_2 / (m_1 + m_2)$ to the reduced mass of the two-body system, with m_1 and m_2 the masses of particles 1 and 2. For the masses of the charmed antimesons and charmed baryons we will take the isospin average of the values listed in the RPP [37].

By particularizing the previous equation for a reference state (mol = ref), we obtain $C_{\text{ref}}^{\text{sat}}$. For $P_\psi^N(4312)$ as the reference state, we find $C_{\text{ref}}^{\text{sat}} = -0.80_{-0.01}^{+0.14} \text{ fm}^2$ for $\Lambda = 1.0$ GeV, where the errors come from the uncertainties in the mass of the $P_\psi^N(4312)$. From this, now we can easily solve the bound state equation for any other (single-channel) molecule simply by making the substitution:

$$1 + 2\mu_{\text{ref}} C_{\text{ref}}^{\text{sat}}(\Lambda) R_{\text{mol}} \int \frac{d^3\vec{q}}{(2\pi)^3} \frac{f^2\left(\frac{q}{\Lambda}\right)}{q^2 + \gamma_{\text{mol}}^2} = 0, \quad (19)$$

where $\gamma_{\text{mol}} = \sqrt{2\mu_{\text{mol}}(M_{\text{th}} - M_{\text{mol}})}$ is the wave number of the bound state, and R_{mol} is the ratio between the relative strength of the coupling for the molecule “mol” and the reference state:

$$R_{\text{mol}} = \frac{\mu_{\text{mol}} C_{\text{mol}}^{\text{sat}}}{\mu_{\text{ref}} C_{\text{ref}}^{\text{sat}}}, \quad (20)$$

which is independent of the unknown proportionality constant in Eq. (16). It is interesting to notice that for our choice of regulator ($f(x) = e^{-x^2}$) the loop integral is analytic and given

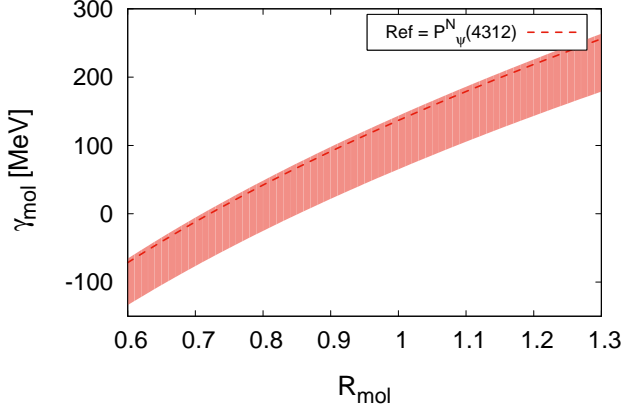


FIG. 1. Dependence of the wave number of a molecule (γ_{mol} , in MeV) on the molecular ratio R_{mol} (defined in Eq. (20)) when the reference state is the $P_{\psi}^N(4312)$. This dependence is calculated by solving Eq. (19) with $\Lambda = 1.0 \text{ GeV}$, $C_{\text{ref}}^{\text{sat}} = -0.80_{-0.01}^{+0.14} \text{ fm}^2$ (given by reproducing the mass of the $P_{\psi}^N(4312)$) and R_{mol} as inputs. The band represents the uncertainty coming from the mass of the reference state. Values of $\gamma_{\text{mol}} > 0$ ($\gamma_{\text{mol}} < 0$) indicate the prediction of a bound (virtual) state.

by

$$\int \frac{d^3 \vec{q}}{(2\pi)^3} \frac{f^2(\frac{q}{\Lambda})}{q^2 + \gamma_{\text{mol}}^2} = \frac{1}{8\pi^2} \left[\sqrt{2\pi} \Lambda - 2 e^{2\gamma_{\text{mol}}^2/\Lambda^2} \pi \gamma_{\text{mol}} \text{erfc} \left(\frac{\sqrt{2}\gamma_{\text{mol}}}{\Lambda} \right) \right], \quad (21)$$

with $\text{erfc}(x)$ the complementary error function. Solutions for which $\gamma_{\text{mol}} > 0$ and $\gamma_{\text{mol}} < 0$ correspond to bound and virtual states, respectively.

Predictions of γ_{mol} only depend on the ratio R_{mol} : $\gamma_{\text{mol}} = \gamma_{\text{mol}}(R_{\text{mol}})$. We show this numerical dependence in Fig. 1 for our cutoff and reference state choices. Bound (virtual) state solutions require:

$$R_{\text{mol}} > 0.72_{-0.01}^{+0.13} \quad (R_{\text{mol}} \leq 0.72_{-0.01}^{+0.13}), \quad (22)$$

where we remind that R_{mol} is defined relative to the reference state $P_{\psi}^N(4312)$ (i.e. other choices of input state will result in different values).

B. Error estimations

We consider four error sources for the calculation of the masses of meson-baryon states:

- (i) the uncertainty of the mass of the reference state, the $P_{\psi}^N(4312)$, which yields $C_{\text{ref}}^{\text{sat}} = -0.80_{-0.01}^{+0.14} \text{ fm}^2$,
- (ii) the uncertainty of the mass of the scalar meson, for which we take $m_S = (475 \pm 75) \text{ MeV}$, i.e., equivalent to the $m_S = (400 - 550) \text{ MeV}$ range listed in the RPP [37],

(iii) the choice of a regularization scale, for which we vary Λ in the $(0.75 - 1.5) \text{ GeV}$ range, where the central value we use — i.e. $\Lambda = 1.0 \text{ GeV}$ — is the harmonic mean of the lower and upper bounds of said range³, and,

(iv) the choice of the parameter α , for which we take $\alpha = 1 \pm 1$. This parameter accounts for the effects of the finite size of the hadrons, with $\alpha = 0$ corresponding to point-like hadrons, while $\alpha > 0$ mimics their finite size.

We notice that the first two sources of uncertainty are external to the model, while the last two correspond to the possible choices of the internal parameters of the model.

For the final error we choose the largest of these sources:

$$\Delta M_{\text{mol}} = \text{minmax} \left\{ M_{\text{mol}}(C_{\text{ref}}^{\text{sat}} \pm \Delta C_{\text{ref}}^{\text{sat}}) - M_{\text{mol}}, \right. \\ M_{\text{mol}}(m_S \pm \Delta m_S) - M_{\text{mol}}, \\ M_{\text{mol}}(\Lambda \pm \Delta \Lambda) - M_{\text{mol}}, \\ \left. M_{\text{mol}}(\alpha \pm \Delta \alpha) - M_{\text{mol}} \right\}, \quad (23)$$

with M_{mol} the central value of the prediction and where “minmax” refers to the maximum (for the positive error) and minimum (for the negative error) number within the list.

C. Coupled channel dynamics

For the molecular pentaquarks in which coupled channel dynamics are required, which happens when there are two nearby meson-baryon thresholds with the same quantum numbers, we will use the previous equation in matrix form

$$\phi_A + \sum_B \phi_B C_{\text{mol}(AB)}^{\text{sat}}(\Lambda) \int \frac{d^3 \vec{q}}{(2\pi)^3} \frac{f^2(\frac{q}{\Lambda})}{M_{\text{th}(B)} + \frac{q^2}{2\mu_B} - M_{\text{mol}}} = 0, \quad (24)$$

where A, B are labels denoting the meson-baryon channels, $M_{\text{th}(B)}$ is the mass of the meson-baryon channel B and ϕ_A, ϕ_B are the vertex functions for channels A, B : ϕ_A is related to the wave function of channel A by means of the relation $(M_{\text{mol}} - \frac{q^2}{2\mu} - M_{\text{th}(A)})\Psi_A(\vec{q}) = \phi_A f(\frac{q}{\Lambda})$. The vertex function ϕ_A is thus related to the coupling of a molecular pentaquark to the meson-baryon channel A . If we write the equations in terms of the relative strength $R_{\text{mol}}^{AB} = \mu_{\text{mol}(B)} C_{\text{mol}}^{\text{sat}(AB)} / (\mu_{\text{ref}} C_{\text{ref}}^{\text{sat}})$, we have

$$\phi_A + 2\mu_{\text{ref}} \sum_B \phi_B C_{\text{ref}}^{\text{sat}}(\Lambda) R_{\text{mol}}^{AB} \int \frac{d^3 \vec{q}}{(2\pi)^3} \frac{f^2(\frac{q}{\Lambda})}{q^2 + \gamma_B^2} = 0, \quad (25)$$

³ This assumes that finite cutoff effects scale as $1/\Lambda$, hence the use of the harmonic mean. Yet, strictly speaking this is only true for a renormalizable contact-range theory, which is not the case, as we are dealing with a phenomenological model that requires Λ to be of the order of the vector meson mass.

where $\gamma_B = \sqrt{2\mu_B(M_{\text{th}(B)} - M_{\text{mol}})}$. For the Gaussian regulator the loop integral is again given by Eq. (21). The coupled channel equations admit solutions with different signs of γ_A , which we will characterize as being in Riemann sheets I ($\gamma_A > 0$) and II ($\gamma_A < 0$).

There are two types of coupled channel dynamics to be considered, namely

- (i) stemming from heavy-quark spin symmetry (HQSS) and,
- (ii) stemming from SU(3)-flavor symmetry.

The first type involves the transition of a ground state heavy hadron into an excited state one, e.g., $\bar{D}\Sigma_c - \bar{D}^*\Sigma_c$ or $\bar{D}^*\Sigma_c - \bar{D}^*\Sigma_c^*$. Within our model this type of dynamics requires the spin-spin or $M1$ component of vector meson exchange, which is weaker than the central or $E0$ component. Besides, the mass splittings involved are usually large. This leads in general to relatively modest effects from HQSS coupled channel dynamics, a point that was explicitly checked with concrete calculations for the pentaquarks in Ref. [30]. We will thus ignore this type of coupled channel dynamics.

The second type involves a transition between two different meson-baryon channels for which there is a common irreducible component of their SU(3)-flavor decomposition (e.g., both channels contain an octet component). To understand this point better, we begin by considering the two types of molecular pentaquarks appearing in this work, the ones containing antitriplet charmed mesons ($T_c = \Lambda_c, \Xi_c$) and the ones containing sextet charmed mesons ($S_c = \Sigma_c, \Xi'_c, \Omega_c$ and $\Sigma_c^*, \Xi_c^*, \Omega_c^*$). We refer to them by the notation $\bar{H}_c T_c$ and $\bar{H}_c S_c$, where $\bar{H}_c = \bar{D}, \bar{D}_s$ and \bar{D}^*, \bar{D}_s^* . From the point of view of SU(3)-flavor symmetry, the $\bar{H}_c T_c$ and $\bar{H}_c S_c$ systems admit, respectively, the decompositions $3 \otimes \bar{3} = 1 \oplus 8$ and $3 \otimes 6 = 8 \oplus 10$. This will give rise to the following subtypes of coupled channel dynamics:

- (a) Most of the $\bar{H}_c S_c$ pentaquarks are pure octets or decuplets and do not mix. The exceptions are the isovector $\bar{D}_s \Sigma_c$ and $\bar{D} \Xi'_c$ and isodoublet $\bar{D}_s \Xi'_c$ and $\bar{D} \Omega_c$ channels, plus the corresponding channels involving the excited charmed antimesons and sextet baryons, for which we have [45]:

$$|\bar{D}_s \Sigma_c\rangle = +\sqrt{\frac{2}{3}}|8\rangle + \frac{1}{\sqrt{3}}|10\rangle, \quad (26)$$

$$|\bar{D} \Xi'_c(1)\rangle = -\frac{1}{\sqrt{3}}|8\rangle + \sqrt{\frac{2}{3}}|10\rangle, \quad (27)$$

$$|\bar{D}_s \Xi'_c\rangle = +\frac{1}{\sqrt{3}}|8\rangle + \sqrt{\frac{2}{3}}|10\rangle, \quad (28)$$

$$|\bar{D} \Omega_c\rangle = -\sqrt{\frac{2}{3}}|8\rangle + \frac{1}{\sqrt{3}}|10\rangle, \quad (29)$$

where the number in parentheses denotes the isospin (if there is any ambiguity) and $|8\rangle$ and $|10\rangle$ denote the SU(3)-flavor irreducible representation. As a consequence, these channels will be coupled. The mass

difference between the thresholds is of the order of 20 MeV, which might justify the explicit inclusion of this effect,

- (b) Most of the $\bar{H}_c T_c$ pentaquarks are pure octets, except for the $\bar{D}_s \Lambda_c$ and isoscalar $\bar{D} \Xi_c$ channels (and the channels involving the excited charmed antimesons), which are a mixture of singlet and octet [45]:

$$|\bar{D}_s \Lambda_c\rangle = \frac{1}{\sqrt{3}}|\tilde{1}\rangle + \sqrt{\frac{2}{3}}|\tilde{8}\rangle, \quad (30)$$

$$|\bar{D} \Xi_c(0)\rangle = \sqrt{\frac{2}{3}}|\tilde{1}\rangle - \frac{1}{\sqrt{3}}|\tilde{8}\rangle, \quad (31)$$

where the notation is analogous to Eqs. (26-29), though we have marked the SU(3)-flavor representations with a tilde to indicate that they are not the same as in the $\bar{H}_c S_c$ case. Again, we will have coupled channel effects. However, the mass difference between these thresholds is about 80 MeV, suggesting this is less important than the $\bar{D} \Xi'_c - \bar{D}_s \Sigma_c$ or $\bar{D}_s \Xi'_c - \bar{D} \Omega_c$ coupled channel dynamics.

- (c) Finally, the octet pieces of the $\bar{H}_c T_c$ and $\bar{H}_c S_c$ pentaquarks can also generate mixing. In our model this effect requires the spin-spin / $M1$ component of vector meson exchange, and it is thus expected to be somewhat weaker when compared to the previously mentioned coupled channel dynamics. Yet, in a few instances the mass difference between the thresholds involved is not particularly large (e.g. the $\bar{D} \Xi_c$ channel with the $\bar{D} \Xi'_c$ or $\bar{D} \Xi_c^*$ channels), making this effect more important than naively expected.

Based on the previous arguments, we expect a hierarchy of coupled channel effects, with (a) being more important than (b) and (c). For the particular case of (b) and (c) their relative size will however depend on the specifics of the thresholds involved (and their mass gaps). Yet, concrete calculations in Ref. [28] indicate that the size of these effects is small except for a few selected molecular configurations (e.g. $\bar{D} \Xi_c(I=1) - \bar{D}_s \Sigma_c$). In the following lines we will elaborate further by calculating the spectrum first in a simplified approach where only type (a) of coupled channel dynamics is included and then in a more complete approach also including the type (b) and (c) dynamics when applicable.

D. Predictions with minimal coupled channel dynamics

In a first approximation we will ignore all the coupled channel dynamics except for the $S = -1, I = 1$ sector of $\bar{H}_c S_c$, i.e. $\bar{D}_s \Sigma_c - \bar{D} \Xi'_c$ and its analogues involving excited charmed antimesons and baryons. That is, we will only consider what we called type (a) coupled channel dynamics in the previous subsection. The coupled channel potential for this sector takes

System	$I(J^P)$	R_{mol}	M_{mol}	Candidate	$M_{\text{candidate}}$
$\Lambda_c \bar{D}$	$\frac{1}{2}(\frac{1}{2}^-)$	0.69	$(4153.6_{-4.9}^{+0.1(B)})^V$	-	-
$\Lambda_c \bar{D}^*$	$\frac{1}{2}(\frac{1}{2}^-, \frac{3}{2}^-)$	0.72	$(4295.0_{-3.6}^{+0.0(B)})^V$	-	-
$\Lambda_c \bar{D}_s$	$0(\frac{1}{2}^-)$	0.86	$4252.5_{-2.0}^{+2.3}$	-	-
$\Lambda_c \bar{D}_s^*$	$0(\frac{1}{2}^-, \frac{3}{2}^-)$	0.89	$4395.2_{-2.3}^{+3.2}$	-	-
$\Xi_c \bar{D}$	$0(\frac{1}{2}^-)$	1.00	$4327.4_{-0.9}^{+6.9}$	$P_{\psi_s}^\Lambda(4338)$	4338.2 ± 0.7
$\Xi_c \bar{D}^*$	$0(\frac{1}{2}^-, \frac{3}{2}^-)$	1.04	$4466.7_{-1.3}^{+7.8}$	$P_{\psi_s}^\Lambda(4459)$	$4458.9_{-3.1}^{+5.5}$
$\Xi_c \bar{D}_s$	$1(\frac{1}{2}^-)$	0.72	$(4336.3_{-3.8}^{+0.0(B)})^V$	-	-
$\Xi_c \bar{D}_s^*$	$1(\frac{1}{2}^-, \frac{3}{2}^-)$	0.74	$4477.6_{-2.4}^{+0.0(V)}$	-	-
$\Xi_c \bar{D}_s$	$\frac{1}{2}(\frac{1}{2}^-)$	0.82	$4436.3_{-2.7}^{+1.2}$	-	-
$\Xi_c \bar{D}_s^*$	$\frac{1}{2}(\frac{1}{2}^-, \frac{3}{2}^-)$	0.85	$4579.2_{-3.3}^{+2.1(V)}$	-	-

TABLE I. Molecular triplet-antitriplet pentaquark states predicted in this work. ‘‘System’’ indicates which charmed antimeson-baryon system we are dealing with, $I(J^P)$ the isospin, spin and parity of the molecule, R_{mol} the molecular ratio (the relative attractiveness of the molecule relative to the $P_\psi^N(4312)$) as defined in Eq. (20), M_{mol} the mass of the molecule, ‘‘Candidate’’ refers to an experimentally observed pentaquark that could correspond with our theoretical prediction and $M_{\text{candidate}}$ to its mass. Masses are expressed in units of MeV. In the M_{mol} column the superscript ‘‘V’’ indicates a virtual state. The errors in M_{mol} come from propagating the uncertainties in the mass of the input or reference state ($P_\psi^N(4312)$), the mass of the scalar meson, the cutoff and the choice of the parameter α and then choosing the largest of them. When the uncertainties allow a state to change from virtual to bound or vice versa, we indicate it by adding (V) or (B) after the upper error.

the generic form

$$V(\bar{D}_s \Sigma_c - \bar{D} \Xi_c') = \begin{pmatrix} \frac{2}{3} V^O + \frac{1}{3} V^D & -\frac{\sqrt{2}}{3} (V^O - V^D) \\ -\frac{\sqrt{2}}{3} (V^O - V^D) & \frac{1}{3} V^O + \frac{2}{3} V^D \end{pmatrix}, \quad (32)$$

$$V(\bar{D}_s \Xi_c' - \bar{D} \Omega_c) = \begin{pmatrix} \frac{1}{3} V^O + \frac{2}{3} V^D & -\frac{\sqrt{2}}{3} (V^O - V^D) \\ -\frac{\sqrt{2}}{3} (V^O - V^D) & \frac{2}{3} V^O + \frac{1}{3} V^D \end{pmatrix}, \quad (33)$$

where V^O and V^D refer to the octet and decuplet potential. In terms of the saturated contact-range couplings, and ignoring in a first approximation the difference among the vector meson masses ($m_\rho, m_\omega, m_{K^*}, m_\phi$), we have

$$V^O = C^O \propto -\frac{g_V g_{V2}}{m_V^2} \left(1 + \kappa_{V1} \kappa_{V2} \frac{m_V^2}{6M^2} \hat{C}_{L12} \right) - \left(\frac{m_V}{m_S} \right)^\alpha \frac{g_S 1 g_{S2}}{m_S^2}, \quad (34)$$

$$V^D = C^D \propto +2 \frac{g_V g_{V2}}{m_V^2} \left(1 + \kappa_{V1} \kappa_{V2} \frac{m_V^2}{6M^2} \hat{C}_{L12} \right) - \left(\frac{m_V}{m_S} \right)^\alpha \frac{g_S 1 g_{S2}}{m_S^2}, \quad (35)$$

where the subindices 1 and 2 indicate the charmed antimeson and charmed sextet baryon, respectively. That is, the octet and decuplet potentials correspond to taking the G-parity and isospin factors $[\zeta + T_{12}] = -1$ and 2 in Eqs. (7), (8) and (16),

System	$I(J^P)$	R_{mol}	M_{mol}	Candidate	$M_{\text{candidate}}$
$\Sigma_c \bar{D}$	$\frac{1}{2}(\frac{1}{2}^-)$	1.00	Input	$P_\psi^N(4312)$	$4311.9_{-0.9}^{+6.8}$
$\Sigma_c^* \bar{D}$	$\frac{1}{2}(\frac{3}{2}^-)$	1.01	$4376.0_{-0.9}^{+7.1}$	-	-
$\Sigma_c \bar{D}^*$	$\frac{1}{2}(\frac{1}{2}^-)$	0.85	$4459.7_{-2.3}^{+2.3}$	$P_\psi^N(4457)$	$4457.3_{-1.8}^{+4.1}$
$\Sigma_c \bar{D}_s^*$	$\frac{1}{2}(\frac{3}{2}^-)$	1.13	$4445.2_{-4.7}^{+10.4}$	$P_\psi^N(4440)$	$4440.3_{-1.8}^{+4.3}$
$\Sigma_c^* \bar{D}^*$	$\frac{1}{2}(\frac{1}{2}^-)$	0.82	$4525.4_{-2.7}^{+1.3(V)}$	-	-
$\Sigma_c^* \bar{D}_s^*$	$\frac{1}{2}(\frac{3}{2}^-)$	0.96	$4520.3_{-1.7}^{+5.3}$	-	-
$\Sigma_c^* \bar{D}_s^*$	$\frac{1}{2}(\frac{3}{2}^-)$	1.19	$4505.8_{-7.5}^{+12.0}$	-	-
$\Xi_c' \bar{D}$	$0(\frac{1}{2}^-)$	1.02	$4435.9_{-0.9}^{+7.3}$	-	-
$\Xi_c^* \bar{D}$	$0(\frac{3}{2}^-)$	1.03	$4502.5_{-1.0}^{+7.5}$	-	-
$\Xi_c' \bar{D}^*$	$0(\frac{1}{2}^-)$	0.88	$4584.2_{-2.7}^{+2.8}$	-	-
$\Xi_c' \bar{D}_s^*$	$0(\frac{3}{2}^-)$	1.16	$4568.8_{-5.8}^{+10.3}$	-	-
$\Xi_c^* \bar{D}^*$	$0(\frac{1}{2}^-)$	0.84	$4652.5_{-3.0}^{+1.7(V)}$	-	-
$\Xi_c^* \bar{D}_s^*$	$0(\frac{3}{2}^-)$	0.98	$4646.9_{-1.8}^{+5.8}$	-	-
$\Xi_c^* \bar{D}_s^*$	$0(\frac{3}{2}^-)$	1.22	$4631.8_{-8.7}^{+12.5}$	-	-
$\Sigma_c \bar{D}_s - \Xi_c' \bar{D}$	$1(\frac{1}{2}^-)$	0.96	$4417.3_{-1.6}^{+4.2}$	-	-
$\Sigma_c^* \bar{D}_s - \Xi_c^* \bar{D}$	$1(\frac{3}{2}^-)$	0.98	$4481.6_{-1.7}^{+4.4}$	-	-
$\Sigma_c \bar{D}_s^* - \Xi_c' \bar{D}^*$	$1(\frac{1}{2}^-)$	0.84	$4581.9_{-2.4}^{+4.4} - (0.6_{-0.5}^{+0.6}) i$	-	-
$\Sigma_c \bar{D}_s^* - \Xi_c^* \bar{D}^*$	$1(\frac{3}{2}^-)$	1.08	$4556.4_{-2.6}^{+7.4}$	-	-
$\Sigma_c^* \bar{D}_s^* - \Xi_c' \bar{D}_s^*$	$1(\frac{1}{2}^-)$	0.81	$4647.4_{-2.5}^{+5.3} - (1.8_{-1.2}^{+2.7}) i$	-	-
$\Sigma_c^* \bar{D}_s^* - \Xi_c^* \bar{D}_s^*$	$1(\frac{3}{2}^-)$	0.94	$4625.5_{-2.6}^{+4.3}$	-	-
$\Sigma_c^* \bar{D}_s^* - \Xi_c^* \bar{D}_s^*$	$1(\frac{3}{2}^-)$	1.13	$4618.6_{-5.1}^{+8.7}$	-	-
$\Xi_c' \bar{D}_s - \Omega_c \bar{D}$	$\frac{1}{2}(\frac{1}{2}^-)$	1.01	$4542.9_{-1.8}^{+3.9}$	-	-
$\Xi_c^* \bar{D}_s - \Omega_c \bar{D}$	$\frac{1}{2}(\frac{3}{2}^-)$	1.02	$4610.0_{-2.0}^{+3.9}$	-	-
$\Xi_c' \bar{D}_s^* - \Omega_c \bar{D}^*$	$\frac{1}{2}(\frac{1}{2}^-)$	0.87	$4699.6_{-2.9}^{+3.8} - (0.5_{-0.3}^{+0.4}) i$	-	-
$\Xi_c' \bar{D}_s^* - \Omega_c \bar{D}_s^*$	$\frac{1}{2}(\frac{3}{2}^-)$	1.13	$4681.0_{-5.1}^{+8.3}$	-	-
$\Xi_c^* \bar{D}_s - \Omega_c \bar{D}_s^*$	$\frac{1}{2}(\frac{1}{2}^-)$	0.84	$4770.8_{-3.5}^{+4.2} - (1.0_{-0.6}^{+0.3}) i$	-	-
$\Xi_c^* \bar{D}_s - \Omega_c \bar{D}_s^*$	$\frac{1}{2}(\frac{3}{2}^-)$	0.97	$4752.0_{-2.7}^{+4.9}$	-	-
$\Xi_c^* \bar{D}_s - \Omega_c \bar{D}_s^*$	$\frac{1}{2}(\frac{3}{2}^-)$	1.19	$4746.3_{-8.1}^{+9.6}$	-	-

TABLE II. Molecular octet pentaquark states predicted in this work. We refer to Table I for the conventions we follow. A complex value of M_{mol} indicates that the state is a resonance, i.e. a pole in the (II, I) Riemann sheet with respect to the lower and higher mass threshold. If there is a V superscript above the complex M_{mol} , this indicates a pole in the (I, II) sheet instead. All binding energies and masses are in units of MeV.

to which we refer for further details. Besides this, when the exchanged vector meson is not the ρ or the ω , we have to correct the previous expressions to take into account the heavier K^* and ϕ masses. To provide a concrete example, we might consider the non-diagonal components of the coupled channel potentials of Eqs. (32) and (33), which require the exchange of a K^* meson, leading to

$$\begin{aligned} V(\bar{D}_s \Sigma_c \rightarrow \bar{D} \Xi_c(1)) &= V(\bar{D}_s \Xi_c \rightarrow \bar{D} \Omega_c) \\ &= -\frac{\sqrt{2}}{3} (V^O - V^D) \\ &\propto \left(\frac{m_V}{m_{K^*}} \right)^\alpha \frac{g_V g_{V2}}{m_{K^*}^2} \left(1 + \kappa_{V1} \kappa_{V2} \frac{m_{K^*}^2}{6M^2} \hat{C}_{L12} \right), \quad (36) \end{aligned}$$

where we remind that $m_V = (m_\rho + m_\omega)/2$.

If we use the $P_\psi^N(4312)$ as the reference state, we obtain the predictions contained in Tables I, II and III. The first set

System	$I(J^P)$	R_{mol}	M_{mol}
$\Sigma_c \bar{D}$	$\frac{3}{2} (\frac{1}{2}^-)$	0.57	$(4316.8_{-27.3}^{+3.9(B)})^V$
$\Sigma_c^* \bar{D}$	$\frac{3}{2} (\frac{3}{2}^-)$	0.58	$(4381.8_{-26.4}^{+3.6(B)})^V$
$\Sigma_c \bar{D}^*$	$\frac{3}{2} (\frac{1}{2}^-)$	0.96	$4455.6_{-1.5}^{+5.4}$
$\Sigma_c^* \bar{D}^*$	$\frac{3}{2} (\frac{3}{2}^-)$	0.41	-
$\Sigma_c^* \bar{D}^*$	$\frac{3}{2} (\frac{1}{2}^-)$	1.07	$4514.6_{-1.9}^{+8.3}$
$\Sigma_c^* \bar{D}^*$	$\frac{3}{2} (\frac{3}{2}^-)$	0.79	$4526.1_{-2.6}^{+0.5(V)}$
$\Sigma_c^* \bar{D}^*$	$\frac{3}{2} (\frac{3}{2}^-)$	0.32	-
$\Sigma_c \bar{D}_s - \Xi_c' \bar{D}$	$1 (\frac{1}{2}^-)$	0.65	$(4445.8_{-2.2(R)}^{+0.0} - (0.1_{-0.1(R)}^{+7.1}) i)^V$
$\Sigma_c^* \bar{D}_s - \Xi_c^* \bar{D}$	$1 (\frac{3}{2}^-)$	0.65	$(4513.0_{-2.2(R)}^{+0.0} - (0.0_{-0.0(R)}^{+6.7}) i)^V$
$\Sigma_c \bar{D}_s^* - \Xi_c' \bar{D}^*$	$1 (\frac{1}{2}^-)$	1.02	$4560.2_{-2.0}^{+4.8}$
$\Sigma_c \bar{D}_s^* - \Xi_c' \bar{D}^*$	$1 (\frac{3}{2}^-)$	0.50	$(4587.5_{-2.4(R)}^{+13.5} - (4.6_{-4.6(R)}^{+22.9}) i)^V$
$\Sigma_c^* \bar{D}_s^* - \Xi_c^* \bar{D}^*$	$1 (\frac{1}{2}^-)$	1.12	$4622.5_{-2.0}^{+6.6}$
$\Sigma_c^* \bar{D}_s^* - \Xi_c^* \bar{D}^*$	$1 (\frac{3}{2}^-)$	0.85	$4651.9_{-3.0}^{+2.3} - (0.0 \pm 0.0) i$
$\Sigma_c^* \bar{D}_s^* - \Xi_c^* \bar{D}^*$	$1 (\frac{3}{2}^-)$	0.42	$(4656.2_{-3.0(R)}^{+24.3} - (9.8_{-9.8(R)}^{+31.6}) i)^V$
$\Xi_c' \bar{D}_s - \Omega_c \bar{D}$	$\frac{1}{2} (\frac{1}{2}^-)$	0.72	$4560.2_{-2.9}^{+4.6} - (1.5_{-1.2}^{+1.0}) i$
$\Xi_c^* \bar{D}_s - \Omega_c \bar{D}$	$\frac{1}{2} (\frac{3}{2}^-)$	0.73	$4630.6_{-2.8}^{+4.3} - (1.5_{-1.2}^{+1.0}) i$
$\Xi_c' \bar{D}_s^* - \Omega_c \bar{D}^*$	$\frac{1}{2} (\frac{1}{2}^-)$	1.07	$4680.3_{-1.8}^{+7.6}$
$\Xi_c' \bar{D}_s^* - \Omega_c \bar{D}^*$	$\frac{1}{2} (\frac{3}{2}^-)$	0.59	$4704.9_{-6.2}^{+18.1} - (4.7_{-2.6}^{+5.3}) i$
$\Xi_c^* \bar{D}_s - \Omega_c \bar{D}$	$\frac{1}{2} (\frac{1}{2}^-)$	1.17	$4742.8_{-5.3}^{+9.9}$
$\Xi_c^* \bar{D}_s - \Omega_c \bar{D}$	$\frac{1}{2} (\frac{3}{2}^-)$	0.92	$4769.3_{-2.7}^{+4.5} - (0.1 \pm 0.0) i$
$\Xi_c^* \bar{D}_s - \Omega_c \bar{D}$	$\frac{1}{2} (\frac{3}{2}^-)$	0.52	$4778.2_{-8.5}^{+27.3} - (6.5_{-3.5}^{+8.6}) i$
$\Omega_c \bar{D}_s$	$0 (\frac{1}{2}^-)$	0.78	$4663.1_{-2.8}^{+0.5(V)}$
$\Omega_c^* \bar{D}_s$	$0 (\frac{3}{2}^-)$	0.79	$4733.6_{-3.0}^{+0.7(V)}$
$\Omega_c \bar{D}_s^*$	$0 (\frac{1}{2}^-)$	1.12	$4792.9_{-3.7}^{+9.2}$
$\Omega_c \bar{D}_s^*$	$0 (\frac{3}{2}^-)$	0.67	$(4807.0_{-13.6}^{+0.4(B)})^V$
$\Omega_c^* \bar{D}_s^*$	$0 (\frac{1}{2}^-)$	1.20	$4857.9_{-7.6}^{+11.5}$
$\Omega_c^* \bar{D}_s^*$	$0 (\frac{3}{2}^-)$	0.98	$4871.4_{-2.8}^{+5.4}$
$\Omega_c^* \bar{D}_s^*$	$0 (\frac{3}{2}^-)$	0.60	$(4875.9_{-30.0}^{+2.2(B)})^V$

TABLE III. Molecular decuplet pentaquark states predicted in this work. We refer to Tables I and II for conventions. However no experimental candidate is known for the decuplet and thus we have not included the columns regarding candidates. If the uncertainties in the mass of a pole originally located in the (I, II) Riemann sheet are able to move it to the (II, I) sheet (i.e. the sheet corresponding to resonances), we will indicate this with the letter (R) following the lower error. All binding energies and masses are in units of MeV.

of predictions — Table I — refers to the $\bar{H}_c T_c$ type of pentaquarks. This includes the $P_{\psi s}^\Lambda(4338)$ and $P_{\psi s}^\Lambda(4459)$, which we predict to be $I = 0 \bar{D}\Xi_c$ and $\bar{D}^*\Xi_c$ bound states with masses of 4327 and 4467 MeV, both within 10 MeV of their experimental masses. The two $\bar{D}^*\Xi_c$ states (with total spin $J = \frac{1}{2}$ and $\frac{3}{2}$, respectively) are degenerate within our choice of coupled channel dynamics. Only when the nearby $\bar{D}\Xi_c'$ and $\bar{D}\Xi_c^*$ channels are included do we obtain a hyperfine splitting between the two spin configurations [10, 28] (we include these channels in the next subsection, where results are shown Table IV), hence reproducing the two peak solution in [2]. It is also worth noticing the prediction of an $I = 1 \bar{D}\Xi_c$ molecule with a mass of 4336 MeV, really close to the experimental mass of the $P_{\psi s}^\Lambda(4338)$, and which might indicate the possible importance of isospin breaking effects and mixing of near threshold $P_{\psi s}^\Lambda$

and $P_{\psi s}^\Sigma$ pentaquarks [6, 7]. There is also a $\bar{D}_s \Lambda_c$ bound state with a mass of 4252 MeV, which is similar to the $P_{\psi s}^\Lambda(4255)$ state predicted in [6] as a flavor partner of the $P_{\psi s}^\Lambda(4338)$ (or in [28] as a flavor and HQSS partner of the $P_{\psi s}^\Lambda(4459)$). Recently, the amplitude analysis of the $J/\psi \Lambda$ invariant mass distribution of [46] also found a $P_{\psi s}^\Lambda(4255)$ pentaquark as a $\bar{D}_s \Lambda_c$ virtual state extremely close to threshold. Meanwhile in [47], which proposes a different phenomenological contact-range potential where the couplings are directly saturated from the light-quark interaction, the existence of a bound $P_{\psi s}^\Lambda(4255)$ is neither confirmed or denied but remains contingent on the choice of couplings (though [47] does not look for virtual state solutions).

Table I also predicts three nucleon-like P_ψ^N states close to threshold: a $P_\psi^N(4154)$, and two $P_\psi^N(4295)$ with spins $J = \frac{1}{2}$, $\frac{3}{2}$ and degenerate masses. The $P_\psi^N(4154)$ might correspond with a possible structure in the $J/\psi \bar{p}$ invariant mass briefly mentioned in [1], though there is a statistical preference for a model without this resonant contribution. Very recently, the new GlueX data [48] for $\gamma p \rightarrow J/\psi p$ shows a dip between the $\bar{D}\Lambda_c$ and $\bar{D}^*\Lambda_c$ thresholds, which in [49] has been interpreted as compatible with a pentaquark signal. The fit in [49] results in a mass of $M = 4235 \pm 8$ MeV, i.e., in between the $P_\psi^N(4154)$ and $P_\psi^N(4295)$ masses. Yet, the analysis of [49] is focused on the compatibility between the GlueX data [48] and the existence of the P_ψ^N pentaquarks already observed by the LHCb, and not on finding new P_ψ^N pentaquarks.

The second set of predictions — Table II — pertains the octet $\bar{H}_c S_c$ pentaquarks. Besides the reference state, the $P_\psi^N(4312)$, other two candidate states are known, the $P_\psi^N(4440)$ and $P_\psi^N(4457)$, which we reproduce as the $J = \frac{3}{2}$ and $J = \frac{1}{2}$ $\bar{D}^*\Sigma_c$ bound states, respectively. Here it is worth commenting that the saturation model provides a very specific prediction of the spin of the $P_\psi^N(4440)$ and $P_\psi^N(4457)$ as molecules, which agrees with other phenomenological molecular models [18, 50] (but not all of them [51]). In contrast compact pentaquark models usually predict the opposite spin identification [25], with the $P_\psi^N(4440)$ and $P_\psi^N(4457)$ being $J = \frac{1}{2}$ and $J = \frac{3}{2}$, respectively. Experimentally, the spins of these two pentaquarks have not been determined yet. There is a fourth P_ψ^N pentaquark candidate that is consistently predicted in most molecular models [15, 18–20] (as a consequence of HQSS) and that a later theoretical analysis of the LHCb $J/\psi p$ data has shown to exist [52], the $P_\psi^N(4380)$. Unsurprisingly (as we incorporate HQSS), our model also reproduces this state. The predictions we obtain for the P_ψ^N pentaquarks are also similar to *scenario B*⁴ in Refs. [15, 17], where a pionless and pionful EFT were used to deduce the $\bar{D}^{(*)}\Sigma_c^{(*)}$ molecular spectrum.

It should be noted that we previously included OPE explicitly for the $\Sigma_c \bar{D}^*$ and $\Sigma_c^* \bar{D}^*$ molecules in Ref. [30] (whose re-

⁴ Scenario A and B refer to the spin of the $P_\psi^N(4440)$ and $P_\psi^N(4457)$ in their interpretation as $\bar{D}^*\Sigma_c$ bound states: A is $J = \frac{1}{2}$ and $\frac{3}{2}$, respectively, while B is the opposite identification. Scenario B is equivalent to the spin prediction in our model.

sults are basically equivalent to the ones presented here ⁵⁾. There we observed that OPE shifts the masses of these pentaquarks by about $(1 - 2)$ MeV; once its sign is taken into account, we end up with

$$M_{\text{OPE}}(\Sigma_c \bar{D}^*, J = \frac{1}{2}) = 4461.3 (4459.7^{+2.3}_{-2.5}) \text{ MeV}, \quad (37)$$

$$M_{\text{OPE}}(\Sigma_c \bar{D}^*, J = \frac{3}{2}) = 4443.6 (4445.2^{+10.4}_{-4.7}) \text{ MeV}, \quad (38)$$

$$M_{\text{OPE}}(\Sigma_c^* \bar{D}^*, J = \frac{1}{2}) = 4526.7 (4525.4^{+1.3(V)}_{-2.7}) \text{ MeV}, \quad (39)$$

$$M_{\text{OPE}}(\Sigma_c^* \bar{D}^*, J = \frac{3}{2}) = 4521.5 (4520.3^{+5.3}_{-1.7}) \text{ MeV}, \quad (40)$$

$$M_{\text{OPE}}(\Sigma_c^* \bar{D}^*, J = \frac{5}{2}) = 4503.3 (4505.8^{+12.0}_{-7.5}) \text{ MeV}, \quad (41)$$

where the number in parentheses is the original calculation without OPE from Table II. It happens that the correction from OPE falls in all cases within the uncertainties of our calculation. For other pentaquarks the mass shifts from OPE are expected to be smaller: in all the other configurations from Tables II and III OPE is not as strong as in the $I = 1/2$ $\Sigma_c \bar{D}^*$ and $\Sigma_c^* \bar{D}^*$ systems. For further details on the calculations with OPE, we refer to Appendix C within [30].

In addition, Table II contains the predictions of a series of $P_{\psi s}^\Lambda$, $P_{\psi s}^\Sigma$ and $P_{\psi ss}^\Xi$ pentaquarks. There are previous molecular predictions of $P_{\psi s}^\Lambda$ pentaquarks [35] and of $P_{\psi s}^\Sigma$ and $P_{\psi ss}^\Xi$ states [53] that are in line with those we obtain here. In particular the comparison with the EFT of Ref. [53] is interesting, as most of our predictions are very similar to scenario B in [53]. The only exceptions are the $J = \frac{1}{2}$ $\bar{D}_s^* \Sigma_c - \bar{D}^* \Xi_c'$ ($\bar{D}_s^* \Xi_c' - \bar{D}^* \Omega_c$) and $\bar{D}_s^* \Sigma_c^* - \bar{D}^* \Xi_c^*$ ($\bar{D}_s^* \Xi_c^* - \bar{D}^* \Omega_c$) pentaquark states (i.e. the four resonances in Table II), for which the decuplet configurations are the most attractive (thus in contradiction with the original assumption made in [53] that the octet was the most attractive configuration, hence the difference). We notice that the idea of a pentaquark octet was previously conjectured in [54], which assumes compact, non-molecular pentaquarks, and it has also appeared in the hadro-charmonium picture [23, 55]. Here it is worth noticing that the predictions of molecular and non-molecular pentaquarks differ in their masses: the mass difference among P_{ψ}^N , $P_{\psi s}^\Lambda$, $P_{\psi s}^\Sigma$ and $P_{\psi ss}^\Xi$ pentaquarks depends on their nature, i.e. if these pentaquarks are observed spectroscopy alone would be able to provide a clue about whether they are molecular or not.

The third set of predictions, shown in Table III, is for the decuplet $\bar{H}_c S_c$ pentaquarks, of which no experimental candidate is known. It is interesting to notice the prediction of a P_{ψ}^Δ molecular pentaquark with a mass of 4456 MeV. This is really close to the $\bar{D}^{*0} \Sigma_c^+$ and $D^{*-} \Sigma_c^{++}$ thresholds, just like the experimental $P_{\psi}^N(4457)$, thus suggesting the possibility of sizable isospin breaking effects, as investigated in [19]. Previous predictions of P_{ψ}^Δ or other decuplet pentaquarks are scarce in the

molecular case, owing to the fact that the electric-type component of vector meson exchange is repulsive, though they appear in the one boson exchange models of [18, 56, 57] (which usually include scalar meson exchange or the tensor components of vector meson exchange).

For the octet and decuplet predictions of Tables II and III, there is the problem of how to distinguish the octet or decuplet nature of a state when there are coupled channel dynamics. This is done by considering the vertex functions ϕ_A (with $A = 1, 2$) for the $\bar{D} \Xi_c' - \bar{D}_s \Sigma_c$ and $\bar{D}_s \Xi_c' - \bar{D} \Omega_c$ family of pentaquarks. For the bound state solutions the relative signs of the vertex functions for the two channels indicate whether we are dealing with an octet or a decuplet (by inverting Eqs. (26-29)). This is not the case though when the pole is above the lower threshold, i.e. when we have a resonance, as the vertex functions become complex numbers. Yet, it happens that for every solution above the lower threshold we have found a second solution below it, from which it is trivial to determine the SU(3)-flavor representation of the resonant solution. To give an example, in the $\bar{D}_s \Xi_c' - \bar{D} \Omega_c$ system we find two poles with masses and vertex functions:

$$M_L = 4542.9 \text{ MeV}, \quad (42)$$

$$(\phi_1, \phi_2)_L = (0.84, -0.54), \quad (43)$$

$$M_H = (4560.2 - 1.5 i) \text{ MeV}, \quad (44)$$

$$(\phi_1, \phi_2)_H = (0.01 - 0.31 i, 0.95), \quad (45)$$

for the lower and higher mass poles (subscripts L and H), respectively. For this system a pure octet configuration corresponds to $(\phi_1, \phi_2) = (\sqrt{2/3}, -\sqrt{1/3}) \simeq (0.82, -0.58)$. From this, it is apparent that the vertex functions of the lower mass pole indicate a predominantly octet state, which we include in Table II. Then, by our convention, the higher mass state is considered to be a decuplet and we include it in Table III.

E. Predictions with extended coupled channel dynamics

The previous predictions can be further improved by including the remaining potentially relevant coupled channel dynamics. The impact of these coupled channel effects is more limited though: they always involve the $\bar{H}_c T_c$ configurations, which are on average lighter than the $\bar{H}_c S_c$ ones. Thus, only a fraction of the $\bar{H}_c S_c$ predictions will be affected.

For what coupled channel dynamics to include, we will follow the detailed analysis of Ref. [28], which quantified the size of coupled channel contributions. Basically there will be eight cases to consider:

- (1) The $J = \frac{1}{2}$ $\bar{D}^* \Lambda_c - \bar{D} \Sigma_c$ potential

$$V(\bar{D}^* \Lambda_c - \bar{D} \Sigma_c) = \begin{pmatrix} \tilde{V}^O & -W^O \\ -W^O & V^O \end{pmatrix}, \quad (46)$$

where \tilde{V}^O and V^O refer to the octet potentials for the $\bar{H}_c T_c$ and $\bar{H}_c S_c$ type of molecular pentaquarks, while

⁵⁾ It is the same model with the same input, the only difference being tiny changes in the charmed meson masses, as Ref. [30] uses a previous version of the RPP. These changes only manifest as truncation errors in the last digit (i.e. as occasional discrepancies of 0.1 MeV in the masses of the pentaquarks).

Channels	System	$I(J^P)$	S	$M_{\text{mol}}^{\text{CC}}$	$\Delta M_{\text{mol}}^{\text{CC}}$	Candidate	$M_{\text{candidate}}$
(1) $\Lambda_c \bar{D}^* - \Sigma_c \bar{D}$	$\Lambda_c \bar{D}^*$	$0(\frac{1}{2}^-)$	0	$4291.0^{+3.9}_{-2.4}$	$-4.0^{(*)}$	-	-
	$\Sigma_c \bar{D}$	$0(\frac{1}{2}^-)$	0	$4315.8^{+5.6}_{-2.3} - (6.6^{+9.6}_{-4.2})i$	+3.9	$P_{\psi}^N(4312)$	$4311.9^{+6.8}_{-0.9} - (4.9^{+2.3}_{-2.6})i$
(2) $\Lambda_c \bar{D}_s - \Xi_c \bar{D}$	$\Lambda_c \bar{D}_s$	$0(\frac{1}{2}^-)$	-1	$4251.8^{+3.0}_{-1.6}$	-0.6	-	-
	$\Xi_c \bar{D}$	$0(\frac{1}{2}^-)$	-1	$4328.1^{+6.4}_{-0.8} - (1.1^{+2.2}_{-0.7})i$	+0.7	$P_{\psi_s}^\Lambda(4338)$	$4338.2 \pm 0.7 - (3.5 \pm 0.6)i$
(3) $\Lambda_c \bar{D}_s^* - \Xi_c' \bar{D} - \Xi_c \bar{D}^*$	$\Lambda_c \bar{D}_s^*$	$0(\frac{1}{2}^-)$	-1	$4393.5^{+4.7}_{-1.3}$	-1.7	-	-
	$\Xi_c' \bar{D}$	$0(\frac{1}{2}^-)$	-1	$4433.6^{+8.8}_{-2.8} - (0.5^{+0.4}_{-0.3})i$	-4.3	-	-
	$\Xi_c \bar{D}^*$	$0(\frac{1}{2}^-)$	-1	$4468.8^{+6.4}_{-1.3} - (3.0^{+5.2}_{-2.0})i$	+1.1	$P_{\psi_s}^\Lambda(4459)$	$4458.9^{+5.5}_{-3.1} - (8.7^{+5.2}_{-4.3})i$
(4) $\Lambda_c \bar{D}_s^* - \Xi_c \bar{D}^* - \Xi_c' \bar{D}$	$\Lambda_c \bar{D}_s^*$	$0(\frac{3}{2}^-)$	-1	$4394.0^{+4.3}_{-1.6}$	-1.2	-	-
	$\Xi_c \bar{D}^*$	$0(\frac{3}{2}^-)$	-1	$4464.6^{+9.1}_{-4.3} - (0.6^{+0.7}_{-0.4})i$	-2.1	$P_{\psi_s}^\Lambda(4459)$	$4458.9^{+5.5}_{-3.1} - (8.7^{+5.2}_{-4.3})i$
	$\Xi_c' \bar{D}$	$0(\frac{3}{2}^-)$	-1	$4503.8^{+6.7}_{-0.9} - (2.0^{+3.5}_{-1.3})i$	+1.3	-	-
(5) $\Sigma_c \bar{D}_s - \Xi_c' \bar{D} - \Xi_c \bar{D}^*$	$\Sigma_c \bar{D}_s - \Xi_c' \bar{D}$ (O)	$1(\frac{1}{2}^-)$	-1	$4415.2^{+5.8}_{-2.4}$	-2.1	-	-
	$\Sigma_c \bar{D}_s - \Xi_c' \bar{D}$ (D)	$1(\frac{1}{2}^-)$	-1	$4446.1^{+1.9}_{-2.0(V)} - (0.1^{+0.4}_{-0.1(V)})i$	+0.3 ^(*)	-	-
	$\Xi_c \bar{D}^*$	$1(\frac{1}{2}^-)$	-1	$(4478.1^{+0.0}_{-2.1} - 0.2^{+11.7}_{-0.2(R)})i^V$	+0.5	-	-
(6) $\Xi_c \bar{D}^* - \Sigma_c \bar{D}_s^* - \Xi_c' \bar{D}$	$\Xi_c \bar{D}^*$	$1(\frac{3}{2}^-)$	-1	$4470.8^{+6.6}_{-4.4}$	-6.8	-	-
	$\Sigma_c \bar{D}_s^* - \Xi_c' \bar{D}$ (O)	$1(\frac{3}{2}^-)$	-1	$(4487.1^{+5.8}_{-2.0(R)} - (0.3^{+11.9}_{-0.3(R)})i)^V$	+5.5 ^(*)	-	-
	$\Sigma_c \bar{D}_s^* - \Xi_c' \bar{D}$ (D)	$1(\frac{3}{2}^-)$	-1	$(4513.4^{+0.9}_{-2.1(R)} - (0.5^{+13.5}_{-0.5(R)})i)^V$	+0.4	-	-
(7) $\Xi_c' \bar{D}_s - \Omega_c \bar{D} - \Xi_c \bar{D}_s^*$	$\Xi_c' \bar{D}_s - \Omega_c \bar{D}$ (O)	$\frac{1}{2}(\frac{1}{2}^-)$	-2	$4540.2^{+6.2}_{-5.0}$	-0.7	-	-
	$\Xi_c' \bar{D}_s - \Omega_c \bar{D}$ (D)	$\frac{1}{2}(\frac{1}{2}^-)$	-2	$4558.6^{+7.6}_{-2.5} - (3.0^{+7.3}_{-2.2})i$	-1.6	-	-
	$\Xi_c \bar{D}_s^*$	$\frac{1}{2}(\frac{1}{2}^-)$	-2	$4580.9^{+5.0}_{-3.6(V)} - (1.1^{+0.1}_{-1.1(V)})i$	+1.7	-	-
(8) $\Xi_c \bar{D}_s^* - \Xi_c' \bar{D}_s - \Omega_c \bar{D}$	$\Xi_c \bar{D}_s^*$	$\frac{1}{2}(\frac{3}{2}^-)$	-2	$4576.2^{+4.7}_{-1.5}$	-3.0	-	-
	$\Xi_c' \bar{D}_s - \Omega_c \bar{D}$ (O)	$\frac{1}{2}(\frac{3}{2}^-)$	-2	$4611.4^{+11.3}_{-3.0} - (1.5^{+1.5}_{-1.4})i$	+1.4	-	-
	$\Xi_c' \bar{D}_s - \Omega_c \bar{D}$ (D)	$\frac{1}{2}(\frac{3}{2}^-)$	-2	$4631.6^{+6.8}_{-3.6} - (1.9^{+0.1}_{-1.6})i$	+1.0	-	-

TABLE IV. Impact of the coupled channel dynamics of Eqs. (46-53) on the molecular pentaquark spectrum. ‘‘Channels’’ indicate the couple channels we are including in the calculation, ‘‘System’’ the charmed antimeson-baryon we are dealing with, $I(J^P)$ the isospin, spin and parity of the system, S the strangeness, $M_{\text{mol}}^{\text{CC}}$ the mass of the molecule, $\Delta M_{\text{mol}}^{\text{CC}}$ is how much the mass of the two-body state changes with respect to the single channel or two channel calculation that we previously considered in Tables I, II and III (it is calculated for the central values only), ‘‘Candidate’’ refers to an experimentally observed pentaquark that could correspond with our theoretical prediction and $M_{\text{candidate}}$ to its mass. In the column ‘‘System’’ the letters in parentheses — O and D — are used to specify whether the state is an octet or decuplet. A complex value of the mass indicates a resonance located in the (II, I, I) or (II, II, I) Riemann sheet (depending on whether it is the middle or the higher mass state, respectively). Meanwhile, if we use the superscript V the pole will be in the (I, II, I) or (I, I, II) sheet. Changes of sheet owing to uncertainties in the location of the state are signaled with ‘‘(V)’’ or ‘‘(R)’’ attached to the lower errors. If the pole has changed sheet as a consequence of the coupled channel dynamics, we indicate it with a $(*)$ superscript in $\Delta M_{\text{mol}}^{\text{CC}}$. Masses are expressed in units of MeV.

W^O denotes the $\bar{H}_c T_c \rightarrow \bar{H}_c S_c$ transition potential (which is always octet).

(2) The $J = \frac{1}{2} \bar{D}_s \Lambda_c - \bar{D} \Xi_c$ potential

$$V(\bar{D}_s \Lambda_c - \bar{D} \Xi_c) = \begin{pmatrix} \frac{1}{3} \tilde{V}^S + \frac{2}{3} \tilde{V}^O & \frac{\sqrt{2}}{3} (\tilde{V}^S - \tilde{V}^O) \\ \frac{\sqrt{2}}{3} (\tilde{V}^S - \tilde{V}^O) & \frac{2}{3} \tilde{V}^S + \frac{1}{3} \tilde{V}^O \end{pmatrix}, \quad (47)$$

where \tilde{V}^S indicates the singlet potential for the $\bar{H}_c T_c$ molecules.

(3) The $J = \frac{1}{2} \bar{D}_s^* \Lambda_c - \bar{D} \Xi_c' - \bar{D}^* \Xi_c$ potential

$$V(\bar{D}_s^* \Lambda_c - \bar{D} \Xi_c' - \bar{D}^* \Xi_c) = \begin{pmatrix} \frac{1}{3} \tilde{V}^S + \frac{2}{3} \tilde{V}^O & -\sqrt{\frac{2}{3}} W^O & \frac{\sqrt{2}}{3} (\tilde{V}^S - \tilde{V}^O) \\ -\sqrt{\frac{2}{3}} W^O & V^O & \frac{1}{\sqrt{3}} W^O \\ \frac{\sqrt{2}}{3} (\tilde{V}^S - \tilde{V}^O) & \frac{1}{\sqrt{3}} W^O & \frac{2}{3} \tilde{V}^S + \frac{1}{3} \tilde{V}^O \end{pmatrix}, \quad (48)$$

(4) The $J = \frac{3}{2} \bar{D}_s^* \Lambda_c - \bar{D}^* \Xi_c - \bar{D} \Xi_c^*$ potential

$$V(\bar{D}_s^* \Lambda_c - \bar{D}^* \Xi_c - \bar{D} \Xi_c^*) = \begin{pmatrix} \frac{1}{3} \tilde{V}^S + \frac{2}{3} \tilde{V}^O & \frac{\sqrt{2}}{3} (\tilde{V}^S - \tilde{V}^O) & -\sqrt{\frac{2}{3}} W^O \\ \frac{\sqrt{2}}{3} (\tilde{V}^S - \tilde{V}^O) & \frac{2}{3} \tilde{V}^S + \frac{1}{3} \tilde{V}^O & \frac{1}{\sqrt{3}} W^O \\ -\sqrt{\frac{2}{3}} W^O & \frac{1}{\sqrt{3}} W^O & V^O \end{pmatrix}, \quad (49)$$

(5) The $J = \frac{1}{2} \bar{D}_s \Sigma_c - \bar{D} \Xi_c' - \bar{D}^* \Xi_c$ potential

$$V(\bar{D}_s \Sigma_c - \bar{D} \Xi_c' - \bar{D}^* \Xi_c) = \begin{pmatrix} \frac{2}{3} V^O + \frac{1}{3} V^D & -\frac{\sqrt{2}}{3} (V^O - V^D) & \sqrt{\frac{2}{3}} W^O \\ -\frac{\sqrt{2}}{3} (V^O - V^D) & \frac{1}{3} V^O + \frac{2}{3} V^D & -\frac{1}{\sqrt{3}} W^O \\ \sqrt{\frac{2}{3}} W^O & -\frac{1}{\sqrt{3}} W^O & \tilde{V}^O \end{pmatrix}, \quad (50)$$

(6) The $J = \frac{3}{2} \bar{D}^* \Xi_c - \bar{D}_s^* \Sigma_c - \bar{D} \Xi_c^*$ potential

$$V(\bar{D}^* \Xi_c - \bar{D}_s^* \Sigma_c - \bar{D} \Xi_c^*) = \begin{pmatrix} \tilde{V}^O & \sqrt{\frac{2}{3}} W^O & -\frac{1}{\sqrt{3}} W^O \\ \sqrt{\frac{2}{3}} W^O & \frac{2}{3} V^O + \frac{1}{3} V^D & -\frac{\sqrt{2}}{3} (V^O - V^D) \\ -\frac{1}{\sqrt{3}} W^O & -\frac{\sqrt{2}}{3} (V^O - V^D) & \frac{1}{3} V^O + \frac{2}{3} V^D \end{pmatrix}, \quad (51)$$

(7) The $J = \frac{1}{2} \bar{D}_s \Xi_c' - \bar{D} \Omega_c - \bar{D}_s^* \Xi_c$ potential

$$V(\bar{D}_s \Xi_c' - \bar{D} \Omega_c - \bar{D}_s^* \Xi_c) = \begin{pmatrix} \frac{1}{3} V^O + \frac{2}{3} V^D & -\frac{\sqrt{2}}{3} (V^O - V^D) & \frac{1}{\sqrt{3}} W^O \\ -\frac{\sqrt{2}}{3} (V^O - V^D) & \frac{2}{3} V^O + \frac{1}{3} V^D & -\sqrt{\frac{2}{3}} W^O \\ \frac{1}{\sqrt{3}} W^O & -\sqrt{\frac{2}{3}} W^O & \tilde{V}^O \end{pmatrix}, \quad (52)$$

(8) The $J = \frac{1}{2} \bar{D}_s^* \Xi_c - \bar{D}_s \Xi_c^* - \bar{D} \Omega_c^*$ potential

$$V(\bar{D}_s^* \Xi_c - \bar{D}_s \Xi_c^* - \bar{D} \Omega_c^*) = \begin{pmatrix} \tilde{V}^O & \frac{1}{\sqrt{3}} W^O & -\sqrt{\frac{2}{3}} W^O \\ \frac{1}{\sqrt{3}} W^O & \frac{1}{3} V^O + \frac{2}{3} V^D & -\frac{\sqrt{2}}{3} (V^O - V^D) \\ -\sqrt{\frac{2}{3}} W^O & -\frac{\sqrt{2}}{3} (V^O - V^D) & \frac{2}{3} V^O + \frac{1}{3} V^D \end{pmatrix}. \quad (53)$$

For the $\bar{H}_c T_c$ molecules, the singlet and octet components of the potential are

$$\tilde{V}^S = \tilde{C}^S \propto -4 \frac{g_{V1} g_{V2}}{m_V^2} - \left(\frac{m_V}{m_S} \right)^\alpha \frac{g_{S1} g_{S2}}{m_S^2}, \quad (54)$$

$$\tilde{V}^O = \tilde{C}^O \propto +2 \frac{g_{V1} g_{V2}}{m_V^2} - \left(\frac{m_V}{m_S} \right)^\alpha \frac{g_{S1} g_{S2}}{m_S^2}, \quad (55)$$

where in this case there is no light-spin dependence. The $\bar{H}_c T_c - \bar{H}_c S_c$ transition component is

$$W^O = E^O \propto -2 \sqrt{3} \frac{g_{V1} g_{V2}}{m_V^2} \kappa_{V1} \kappa_{V2} \frac{m_V^2}{6M^2} \hat{C}_{L12}, \quad (56)$$

which is purely magnetic-like ($M1$), with $\kappa_{V2} = \frac{3}{2} (\mu_u / \mu_N)$ for the $\Xi_c \rightarrow \Xi_c^{(*)}$ transitions [10], and where the value of the spin-spin operator always happens to be one, $\hat{C}_{L12} = 1$.

For the calculation of the spectrum with the extended coupled channels, we will use the $P_\psi^N(4312)$ as the reference state, but still in the single channel approximation. The reason for not updating the input to its coupled channel version is the following: if we recalculate the $P_\psi^N(4312)$ with the coupled channel dynamics of Eq. (46) and the single channel reference coupling $C_{\text{ref}}^{\text{sat}} = -0.80_{-0.01}^{+0.14} \text{ fm}^2$, we now predict the mass of the $P_\psi^N(4312)$ to be

$$M(\bar{D} \Sigma_c) = 4315.8_{-2.3}^{+4.8} - (6.6_{-4.2}^{+8.2}) i \text{ MeV}, \quad (57)$$

which is compatible with the experimental mass and width of the $P_\psi^N(4312)$ within errors ($M_{\text{exp}} - (\Gamma_{\text{exp}}/2) i = [4311.9_{-0.9}^{+6.8} - (4.9_{-2.6}^{+2.3}) i] \text{ MeV}$). As a consequence it is not necessary (within the accuracy of the theory or the experiment) to recalibrate the input.

With the previous choice, the predictions of the states affected by the extended coupled channel dynamics of Eqs. (46-53) are presented in Table IV. Within this Table we include the calculation of the mass shift generated by the coupled channel dynamics, $\Delta M_{\text{mol}}^{\text{CC}}$ in Table IV. It is interesting to notice that this mass shift is in general smaller in magnitude than the uncertainties we previously calculated in Tables I, II and III. There are exceptions though to this rule: the most notable one is the $I = 1, J = \frac{3}{2} \Xi_c \bar{D}^*$ state — a $P_{\psi_s}^\Sigma$ pentaquark — which becomes about 7 MeV more bound than in the single channel calculation. Other example is the $I = 0, J = \frac{1}{2} \Lambda_c \bar{D}^*$ state — a P_ψ^N pentaquark — which before was a virtual state basically at threshold and now is a bound state a few MeV below threshold. Regarding the $P_{\psi_s}^\Lambda(4459)$ pentaquark, the inclusion of the coupled channel dynamics generates a certain degree of hyperfine splitting between the $J = \frac{1}{2}$ and $\frac{3}{2} \Xi_c \bar{D}^*$ configurations ($|\Delta M| = 4.2 \text{ MeV}$), though of a smaller magnitude than the double peak solution in [2] ($|\Delta M_{\text{exp}}| = 12.9 \pm 4.6 \text{ MeV}$).

F. Isospin breaking effects

Within the previous set of predictions it is not rare to find a few states close to a threshold, opening the possibility of isospin breaking effects when the relevant threshold can be decomposed into two nearby particle states with the same third component of their total isospin. Examples are the $P_{\psi_s}^\Sigma(4336)$ molecule predicted in Table I or the $P_\psi^N(4460)$ and $P_\psi^\Lambda(4456)$ molecules of Tables II and III, which are experimentally relevant owing to their possible relation with the $P_{\psi_s}^\Lambda(4338)$ and $P_\psi^N(4457)$ states.

Here we consider the isospin breaking of the thresholds for the particular cases of the $\Xi_c \bar{D}$ system and a few selected configurations of the $\Sigma_c^{(*)} \bar{D}^{(*)}$ molecules. The inclusion of these effects is straightforward:

(a) First, we split the $\Xi_c \bar{D}$ and $\Sigma_c^{(*)} \bar{D}^{(*)}$ systems into the $\Xi_c^0 \bar{D}^0 - \Xi_c^+ D^-$ and $\Sigma_c^{(*)+} \bar{D}^{(*)0} - \Sigma_c^{(*)++} D^{(*)-}$ channels, respectively.

System	$I(J^P)$	M_{mol}	$I(J^P)$	M_{mol}	Candidate	$M_{\text{candidate}}$
$\Xi_c^0 \bar{D}^0 - \Xi_c^+ D^-$	$0 (\frac{1}{2}^-)$	$4327.3^{+6.7}_{-0.9}$	$1 (\frac{1}{2}^-)$	$4337.3^{+4.7}_{-2.3} - (0.9^{+0.0}_{-0.9(B/V)}) i$	$P_{\psi_s}^\Lambda(4338)$	4338.2 ± 0.7
$\Sigma_c^{*+} D^- - \Sigma_c^+ \bar{D}^0$	$\frac{1}{2} (\frac{1}{2}^-)$	$4312.2^{+5.3}_{-0.9}$	$\frac{3}{2} (\frac{1}{2}^-)$	$4325.6^{+7.1}_{-4.1} - (3.9^{+4.8}_{-2.4}) i$	$P_{\psi}^N(4312)$ $P_{\psi}^N(4337)$	$4311.9^{+6.8}_{-0.9}$ 4337^{+7}_{-5}
$\Sigma_c^{*++} D^- - \Sigma_c^{*+} \bar{D}^0$	$\frac{1}{2} (\frac{3}{2}^-)$	$4376.3^{+5.9}_{-0.9}$	$\frac{3}{2} (\frac{3}{2}^-)$	$4390^{+7.4}_{-4.3} - (4.0^{+4.9}_{-2.2}) i$	-	-
$\Sigma_c^{*+} D^{*-} - \Sigma_c^+ \bar{D}^{*0}$	$\frac{1}{2} (\frac{1}{2}^-)$	$4461.1^{+3.0}_{-2.5} - (0.2^{+0.2}_{-0.2(B)}) i$	$\frac{3}{2} (\frac{1}{2}^-)$	$4453.9^{+4.9}_{-1.6}$	$P_{\psi}^N(4457)$	$4457.3^{+4.1}_{-1.8}$
$\Sigma_c^{*++} D^{*-} - \Sigma_c^{*+} \bar{D}^{*0}$	$\frac{1}{2} (\frac{1}{2}^-)$	$(4526.3 \pm 2.7) - (0.5^{+0.2}_{-0.5(B)}) i$	$\frac{3}{2} (\frac{1}{2}^-)$	$4513.3^{+8.1}_{-1.8}$	-	-
$\Sigma_c^{*++} D^{*-} - \Sigma_c^{*+} \bar{D}^{*0}$	$\frac{1}{2} (\frac{3}{2}^-)$	$4520.1^{+4.1}_{-1.9}$	$\frac{3}{2} (\frac{3}{2}^-)$	$4525.9^{+2.6}_{-2.5} - (0.7^{+0.8}_{-0.7(B)}) i$	-	-

TABLE V. Selection of molecular pentaquark states for which the isospin breaking effects are worth considering. ‘‘System’’ indicates which charmed antimeson-baryon we are dealing with, $I(J^P)$ the isospin, spin and parity of the molecule, R_{mol} the molecular ratio (the relative attractiveness of the molecule relative to the $P_{\psi}^N(4312)$) as defined in Eq. (20), M_{mol} the mass of the molecule, ‘‘Candidate’’ refers to an experimentally observed pentaquark that could correspond with our theoretical prediction and $M_{\text{candidate}}$ to its mass. Masses are expressed in units of MeV. In the M_{mol} column the superscript ‘‘V’’ indicates a virtual state. The errors in M_{mol} are calculated as in Table I. When the uncertainties allow a state to change from virtual to bound or vice versa, we indicate it by adding (V) or (B) after the upper error.

(b) Second, we substitute the isospin operator by

$$T_{12} \rightarrow \begin{pmatrix} -1 & +2 \\ +2 & -1 \end{pmatrix} \text{ for } \Xi_c^0 \bar{D}^0 - \Xi_c^+ D^-, \quad (58)$$

$$T_{12} \rightarrow \begin{pmatrix} 0 & +\sqrt{2} \\ +\sqrt{2} & -1 \end{pmatrix} \text{ for } \Sigma_c^{(*)+} \bar{D}^{(*)0} - \Sigma_c^{(*)++} D^{(*)-}, \quad (59)$$

in Eq. (16), which now becomes a coupled channel equation, while every other operator remains diagonal in the particle basis.

Then we recalculate the spectrum in Table V, where we classify states into approximate isospin representations by adapting the criterion we already used for SU(3)-flavor breaking to isospin. That is, we inspect the vertex functions ϕ_A (with $A = 1, 2$) of the states that are below threshold in the particle basis and compare them with their expected value in the absence of isospin breaking. For instance, in the $\Xi_c^0 \bar{D}^0 - \Xi_c^+ D^-$ system we obtain two poles with masses and vertex functions:

$$M_L = 4327.4 \text{ MeV}, \quad (60)$$

$$(\phi_1, \phi_2)_L = (0.74, -0.68), \quad (61)$$

$$M_H = (4337.3 - 0.9 i) \text{ MeV}, \quad (62)$$

$$(\phi_1, \phi_2)_H = (0.35 - 0.40 i, 0.85), \quad (63)$$

for the lower and higher mass poles (subscripts L and H), respectively. In the isospin symmetric limit, the $\Xi_c \bar{D}$ system can be in the $I = 0, 1$ configurations, where for $I = 0$ we expect the vertex functions to be $(\phi_1, \phi_2) = (1/\sqrt{2}, -1/\sqrt{2}) \simeq (0.71, -0.71)$ in the particle basis. From this we conclude that the lower mass pole is predominantly $I = 0$ and classify the higher mass pole as $I = 1$.

The spectrum of Table V is worth commenting in more detail owing to its possible connection with experimental observations:

- (i) In the $\Xi_c \bar{D}$ system, the mass of the $I = 1$ state is really close to the one of the $P_{\psi_s}^\Lambda(4338)$ pentaquark, which begs the question of whether this peak is actually a $P_{\psi_s}^{\Sigma^0}$

or a combination of the two peaks we predict. This is not impossible if we take into account that isospin breaking effects allow both the $P_{\psi_s}^\Lambda$ and $P_{\psi_s}^{\Sigma^0}$ to decay into $J/\Psi \Lambda$ (instead of only $P_{\psi_s}^\Lambda$ if isospin is not broken).

However, the analysis of Ref. [46], which includes both the $\Xi_c^0 \bar{D}^0$ and $\Xi_c^+ D^-$ channels, prefers a $P_{\psi_s}^\Lambda$ -type solution (i.e. $I = 0$), which happens to be above both these thresholds. This corresponds to a $\Xi_c \bar{D}$ system somewhat less attractive than what we find in our model.

- (ii) In the $\Sigma_c \bar{D}$ system the $I = 3/2$ P_{ψ}^Δ molecule, which was a virtual state in the isospin symmetric limit, is now a resonance above the $\Sigma_c^+ \bar{D}^0$ and $\Sigma_c^{*+} D^-$ thresholds. Its mass is similar to that of the $P_{\psi}^N(4337)$ [27], a pentaquark whose nature remains obscure [28, 29]. This similarity in the masses invites the re-interpretation of the $P_{\psi}^N(4337)$ as a possible P_{ψ}^Δ molecular pentaquark, instead of the less exotic P_{ψ}^N interpretation. However, this explanation is contingent on two factors: first, that the spin and parity of the $P_{\psi}^N(4337)$ are $J^P = \frac{1}{2}^-$ (instead of the preferred $J^P = \frac{1}{2}^+$ [27]) and second, that there is destructive interference in the $B_s^0 \rightarrow J/\Psi p \bar{p}$ between the contributions from the P_{ψ}^N and $P_{\psi}^{\bar{N}}$ – i.e. the $I = 1/2$ $\Sigma_c \bar{D}$ and $\bar{\Sigma}_c D$ molecular pentaquarks – while the contributions from the $I = 3/2$ P_{ψ}^Δ and $P_{\psi}^{\bar{\Delta}}$ states interfere constructively. As a reminder, it is interesting to notice that the experimental analysis from which the properties of the P_{ψ}^N were determined assumes the existence of just one pentaquark in the vicinity of the 4337 MeV mass range [27].

- (iii) For the $J = 1/2$ $\Sigma_c \bar{D}^*$ system there was already more attraction in the $I = 3/2$ configuration than in the $I = 1/2$ one in the isospin symmetric limit. The inclusion of isospin breaking effects makes the P_{ψ}^Δ a bit more bound, while pushing the P_{ψ}^N above the $\Sigma_c^+ \bar{D}^{*0}$ threshold. This is relevant for the interpretation of the $P_{\psi}^+(4457)$ pentaquark, which is usually considered to be $I = 1/2$ and have the quantum numbers of a pro-

ton. But once isospin breaking is taken into account, its interpretation as a mostly $I = 3/2$ P_ψ^Δ state is more natural from the point of view of spectroscopy⁶. Yet, this is not the only reason in favor of the $I = 3/2$ hypothesis: this option also explains better the *production fractions* of the LHCb pentaquarks⁷. If the $P_\psi(4457)$ were to be a $J = 1/2$, $I = 1/2$ $\Sigma_c \bar{D}$ molecule, its production fraction could be expected to be one order of magnitude larger than the experimental one [63, 64]. In contrast, with the spectrum obtained in Table II for the $P_\psi^N(4440)$ and Table V for the $P_\psi^N(4312)$ and the prospective $P_\psi^\Delta(4457)$, the calculation of the relative production fractions (check Ref. [64] for a detailed explanation) yields

$$1 : 1.67 \mathcal{R}_2 : 0.86 \mathcal{R}_3 [11.5 \mathcal{R}_3], \quad (65)$$

for $P_\psi^N(4312)$, $P_\psi^N(4440)$ and $P_\psi^\Delta(4457)$ [$P_\psi^N(4457)$], respectively, where \mathcal{R}_2 and \mathcal{R}_3 are the ratios of the $\mathcal{B}(\Lambda_b^0 \rightarrow K^- P_c^+)$ branching ratios for the $P_c^+ = P_\psi^N(4440)$ and $P_\psi^\Delta(4457)$ [$P_\psi^N(4457)$] relative to $P_\psi^N(4312)$. In the calculation above we are not using the physical pentaquark masses, but instead their predictions within our RG-saturation model: the $P_\psi^N(4312)$ and $P_\psi^\Delta(4457)$ are the ones calculated in Table V, while the $P_\psi^N(4440)$ corresponds to Table II. The number within the square brackets represents the ratio for the $P_\psi^\Delta(4457)$ as calculated from the mass of the molecular prediction in Table II. For comparison, the experimental values are [3]

$$1 : 3.7_{-2.3}^{+2.5} : (1.8 \pm 1.2), \quad (66)$$

which are compatible with our determination provided \mathcal{R}_2 and \mathcal{R}_3 are of natural size. In contrast, for the $P_\psi^N(4457)$ of Table II the ratio \mathcal{R}_3 needs to be rather small.

⁶ Had we considered the effect of the nearby $\Lambda_{c1}(2595)\bar{D}$ threshold (a possibility which has been discussed in the literature [58–62]), with a mass of 4459.5 and thus below the prediction of the $J = 1/2$, $I = 1/2$ $\Sigma_c \bar{D}^*$ in Table V (i.e. 4461.1 MeV), this effect would have further increased the mass of the P_ψ^N , making it a less likely interpretation of the $P_\psi^N(4457)$. However, the $\Sigma_c \bar{D}^* - \Lambda_{c1}(2595)\bar{D}$ dynamics involve P-wave interactions, for which our saturation model does not apply (as it is constrained to the S-wave case).

⁷ Here by production fractions we refer to the following ratio of branching ratios:

$$\mathcal{F}(P_\psi) = \frac{\mathcal{B}(\Lambda_b^0 \rightarrow K^- P_\psi^+) \mathcal{B}(P_\psi^+ \rightarrow J/\Psi p)}{\mathcal{B}(\Lambda_b^0 \rightarrow K^- J/\Psi p)}, \quad (64)$$

where \mathcal{B} are the branching ratios of the particular decays considered. Experimentally, for the $P_\psi^+(4312/4440/4457)$ pentaquarks we have $\mathcal{F} = 0.30_{-0.11}^{+0.35}$, $1.11_{-0.34}^{+0.40}$, $0.53_{-0.21}^{+0.22}$, respectively [3] (notice that we have removed the N superscripts in the pentaquarks to indicate that we are not making any assumptions about their isospin). Alternatively, if we want to compare the relative production ratios, we might divide by $\mathcal{F}(P_\psi(4312))$, yielding 1 , $3.7_{-2.3}^{+2.5}$ and 1.8 ± 1.2 .

System	$I(J^P)$	R'_{mol}	M'_{mol}	Candidate	$M_{\text{candidate}}$
$\Lambda_c \bar{D}_s$	$0(\frac{1}{2}^-)$	0.86	$(4253.1^{+1.0}_{-2.3})^V$	-	-
$\Lambda_c \bar{D}_s^*$	$0(\frac{1}{2}^-, \frac{3}{2}^-)$	0.89	$(4397.7^{+0.7}_{-1.8})^V$	-	-
$\Xi_c \bar{D}$	$0(\frac{1}{2}^-)$	1.00	4336.3 (Input)	$P_{\psi_s}^\Delta(4338)$	4338.2 ± 0.7
$\Xi_c \bar{D}^*$	$0(\frac{1}{2}^-, \frac{3}{2}^-)$	1.04	$4477.5^{+0.1}_{-0.2}$	$P_{\psi_s}^\Delta(4459)$	$4458.9^{+5.5}_{-3.1}$
$\Sigma_c \bar{D}$	$\frac{1}{2}(\frac{1}{2}^-)$	1.00	$(4320.7 \pm 0.0)^V$	$P_\psi^N(4312)$	$4311.9^{+6.8}_{-0.9}$
$\Sigma_c^* \bar{D}$	$\frac{1}{2}(\frac{3}{2}^-)$	1.01	4385.3 ± 0.0	-	-
$\Sigma_c \bar{D}^*$	$\frac{1}{2}(\frac{1}{2}^-)$	0.86	$(4460.3^{+1.2}_{-3.2})^V$	$P_\psi^N(4457)$	$4457.3^{+4.1}_{-1.8}$
$\Sigma_c \bar{D}^*$	$\frac{1}{2}(\frac{3}{2}^-)$	1.13	$4460.9^{+0.5}_{-1.5}$	$P_\psi^N(4440)$	$4440.3^{+4.3}_{-1.8}$
$\Sigma_c^* \bar{D}^*$	$\frac{1}{2}(\frac{1}{2}^-)$	0.82	$(4524.0^{+2.0}_{-5.3})^V$	-	-
$\Sigma_c^* \bar{D}^*$	$\frac{1}{2}(\frac{3}{2}^-)$	0.96	$(4526.5^{+0.1}_{-0.5})^V$	-	-
$\Sigma_c \bar{D}^*$	$\frac{1}{2}(\frac{3}{2}^-)$	1.19	$4524.4^{+1.0}_{-2.8}$	-	-

TABLE VI. Selection of molecular pentaquark states when the $P_{\psi_s}^\Delta(4338)$ is chosen as the reference state (with the caveat that we describe it as an isoscalar $\bar{D}\Xi_c$ bound state at threshold). We refer to Table I for the conventions we follow, where the only change is the addition of a prime to R'_{mol} and M'_{mol} with the intention of indicating that the molecular ratios and masses are now derived from the $P_{\psi_s}^\Delta(4338)$. The uncertainties shown here only take into account the mass of the scalar meson, the cutoff choice and the parameter α . All binding energies and masses are in units of MeV.

- (iv) For the $\Sigma_c^* \bar{D}^*$ system, we find two states above the $\Sigma_c^+ \bar{D}^{0*}$ threshold: a $J = 1/2$ P_ψ^N and $J = 3/2$ P_ψ^Δ . The $I = 3/2$ molecule might in turn be related with a possible $I = 3/2$ structure with a mass in the (4545 – 4553) MeV range recently observed in the $\Lambda_c^+ D^- \pi^-$ decay channel by the LHCb [65] (though with a poor local significance, ranging from (1.9 – 3.6) σ depending on the assumed width).

We remind that the present analysis can be easily extended to other pentaquarks close to a threshold, which could come in handy if future experimental observations find this type of states. For the moment, though, we have limited the explicit inclusion of isospin breaking to the pentaquarks were it might be empirically relevant.

G. Using the $P_{\psi_s}^\Delta(4338/4459)$ as the reference state

Finally we consider the question of how predictions change if a different reference state is chosen. Ideally, the reference state should have a straightforward molecular interpretation and, if possible, be also well-established experimentally. This leaves us with five possible candidates: the $P_\psi^N(4312/4440/4457)$ and the $P_{\psi_s}^\Delta(4338/4459)$ (though, of the strange pentaquarks, only the $P_{\psi_s}^\Delta(4338)$ surpasses the 5σ discovery threshold). However, the three non-strange pentaquarks are known to be consistently described with similar parameters [15, 19]. In terms of the RG-improved saturation model this manifests as the fact that the predictions for the masses of the $P_\psi^N(4440)$ and $P_\psi^N(4457)$ obtained from the $P_\psi^N(4312)$ are compatible with the experimental ones, as can be checked in Table II. In this case changing the reference

System	$I(J^P)$	R''_{mol}	M''_{mol}	Candidate	$M_{\text{candidate}}$
$\Lambda_c \bar{D}_s$	$0 (\frac{1}{2}^-)$	0.82	$4248.5^{+3.4}_{-3.1}$	-	-
$\Lambda_c \bar{D}_s^*$	$0 (\frac{1}{2}^-, \frac{3}{2}^-)$	0.85	$4390.8^{+3.8}_{-3.4}$	-	-
$\Xi_c \bar{D}$	$0 (\frac{1}{2}^-)$	0.96	$4320.2^{+5.1}_{-2.9}$	$P_{\psi_s}^\Lambda(4338)$	4338.2 ± 0.7
$\Xi_c \bar{D}^*$	$0 (\frac{1}{2}^-, \frac{3}{2}^-)$	1.00	Input	$P_{\psi_s}^\Lambda(4459)$	$4458.9^{+5.5}_{-3.1}$
$\Sigma_c \bar{D}$	$\frac{1}{2} (\frac{1}{2}^-)$	0.96	$4304.8^{+5.1}_{-2.9}$	$P_{\psi}^N(4312)$	$4311.9^{+6.8}_{-0.9}$
$\Sigma_c^* \bar{D}$	$\frac{1}{2} (\frac{3}{2}^-)$	0.97	$4368.7^{+5.2}_{-2.9}$	-	-
$\Sigma_c \bar{D}^*$	$\frac{1}{2} (\frac{1}{2}^-)$	0.82	4455.9 ± 4.0	$P_{\psi}^N(4457)$	$4457.3^{+4.1}_{-1.8}$
$\Sigma_c \bar{D}^*$	$\frac{1}{2} (\frac{3}{2}^-)$	1.09	$4435.6^{+6.8}_{-4.2}$	$P_{\psi}^N(4440)$	$4440.3^{+4.3}_{-1.8}$
$\Sigma_c^* \bar{D}^*$	$\frac{1}{2} (\frac{1}{2}^-)$	0.79	$4522.4^{+3.7}_{-4.5}$	-	-
$\Sigma_c^* \bar{D}^*$	$\frac{1}{2} (\frac{3}{2}^-)$	0.92	$4514.4^{+4.3}_{-2.5}$	-	-
$\Sigma_c^* \bar{D}^*$	$\frac{1}{2} (\frac{3}{2}^-)$	1.14	$4495.1^{+7.5}_{-6.8}$	-	-

TABLE VII. Same as Table VI but using the $P_{\psi_s}^\Lambda(4459)$ as a reference state, where the only change is the addition of a second prime to R''_{mol} and M''_{mol} to distinguish them from the molecular ratios and masses obtained from the other input choices. The uncertainties here include the error in the mass of the reference state, in addition to the other three error sources (m_σ , Λ , α). All binding energies and masses are in units of MeV.

state from the $P_{\psi}^N(4312)$ to any of the other two will not significantly alter the predictions.

The situation is different though with the $P_{\psi_s}^\Lambda(4338)$ and $P_{\psi_s}^\Lambda(4459)$ pentaquarks, which overbinds and underbinds respectively in our model if the $P_{\psi}^N(4312)$ is used as input (see Table I). Thus, it is worth exploring how predictions change if we use the $P_{\psi_s}^\Lambda(4338/4459)$ pentaquarks as the reference state.

The only difficulty is that if we use the $P_{\psi_s}^\Lambda(4338)$ as input its mass is above the $\Xi_c \bar{D}$ threshold, which is not reproducible in a single channel calculation. Actually, even after the inclusion of coupled channel effects, it is still not possible to obtain the mass of the $P_{\psi_s}^\Lambda(4338)$: if we consider isospin breaking effects, the $\Xi_c^0 \bar{D}^0 - \Xi_c^+ D^-$ coupled channel dynamics is able to generate an isovector $P_{\psi_s}^\Sigma$ molecule above threshold, but not an isoscalar $P_{\psi_s}^\Lambda$ one. Conversely, if we consider the $\Lambda_c \bar{D}_s - \Xi_c \bar{D}$ coupled channel dynamics, the transition potential is able to generate a resonance barely above threshold, but not above enough as to reproduce the Breit-Wigner mass of the $P_{\psi_s}^\Lambda(4338)$ (for that we will need a stronger transition potential than the one generated by K^* -exchange in our model).

In view of the previous limitations, we will model the $P_{\psi_s}^\Lambda(4338)$ as a $I = 1/2 \Xi_c \bar{D}$ bound state at threshold, i.e. $M_{\text{th}} = 4336.3 \text{ MeV}$ in the isospin symmetric limit (for which $C_{\text{mol}}^{\text{sat}} = -0.58 \text{ fm}^2$ for $\Lambda = 1.0 \text{ GeV}$). To keep matters simple, we will concentrate on the most experimentally relevant sectors: the $\Lambda_c \bar{D}_s^{(*)}$ (for which there are predictions of a partner of the $P_{\psi_s}^\Lambda(4338)$ [6, 46]), $I = 0 \Xi_c \bar{D}^{(*)}$ and $I = 1/2 \Sigma_c^{(*)} \bar{D}^{(*)}$ systems, where the new predictions are presented in Table VI. The most evident difference with the predictions derived from the $P_{\psi}^N(4312)$ is the reduced attraction, which disfavors the formation of bound states (but favors virtual states). Curiously, the molecular ratios R'_{mol} with the new input are identical to the previous ones, where the reason is that the $\mu_{\text{mol}} C_{\text{mol}}^{\text{sat}}$

of the $P_{\psi}^N(4312)$ and $P_{\psi_s}^\Lambda(4338)$ differ by only a 0.3%, smaller than the accuracy with which they are listed in Table VI. From this coincidence it can be inferred that only the molecules for which $R_{\text{mol}} > 1.0$ when the $P_{\psi}^N(4312)$ was used as input will survive as bound states when the $P_{\psi_s}^\Lambda(4338)$ is the reference state.

It is worth noticing that neither the mass of the $P_{\psi_s}^\Lambda(4459)$ nor the masses of the $P_{\psi}^N(4312/4440/4457)$ pentaquarks are reproduced in Table VI. This either suggests that the $P_{\psi_s}^\Lambda(4338)$ is not a bound state or, if it is indeed molecular, that its Breit-Wigner mass does not correspond with the mass of the pole in $\Xi_c \bar{D}$ scattering. Nonetheless this is a common occurrence with molecular states that has been extensively discussed in the literature [66–68].

If we use instead the $P_{\psi_s}^\Lambda(4459)$ as the reference state (where it is described as a $\Xi_c \bar{D}^*$ molecule with $I = 0$, yielding $C_{\text{ref}}^{\text{sat}} = -0.89^{+0.09}_{-0.06} \text{ fm}^2$ at $\Lambda = 1.0 \text{ GeV}$), we obtain the molecular spectrum of Table VII. In this case the predicted masses of the pentaquarks are usually lighter than their Breit-Wigner masses, though for the $P_{\psi}^N(4440/4457)$ they are still compatible with the experimental values within uncertainties. In contrast, the $P_{\psi_s}^\Lambda(4338)$ and $P_{\psi}^N(4312)$ overbind: the incompatibility with the $P_{\psi_s}^\Lambda(4338)$ is particularly worrying, as it should have the same potential as the $P_{\psi_s}^\Lambda(4459)$ (at least, if both are isoscalar molecules). However here it should be noted that the experimental evidence for the $P_{\psi_s}^\Lambda(4459)$ is less conclusive than for its low mass partner. Future observations might change its mass, or its single-/double-peak nature, which in turn will help us to update the predictions in our model.

IV. CONCLUSIONS

We have predicted the molecular hidden-charm pentaquark spectrum within a compact theoretical description of the baryon-antimeson interaction in terms of a contact-range S-wave potential. The couplings of this potential are saturated by the exchange of light-mesons (σ , ρ , ω), where a few renormalization group ideas are included to properly combine the contributions from mesons with different ranges. The couplings thus obtained are unique except for an unknown proportionality constant, which can be easily determined from a reference or input state.

If we use the $P_{\psi}^N(4312)$ as input (assuming it to be a $\bar{D} \Sigma_c$ bound state), we are able to approximately reproduce the masses of the $P_{\psi}^N(4440)$ and $P_{\psi}^N(4457)$ as $J = \frac{3}{2}$ and $\frac{1}{2} \bar{D}^* \Sigma_c$ bound states, as well as the theorized narrow $P_{\psi}^N(4380)$ [15, 18, 19, 52]. The extension of this model to the molecular pentaquarks containing an antitriplet charmed baryon predicts the existence of $\bar{D} \Xi_c$ and $\bar{D}^* \Xi_c$ $P_{\psi_s}^\Lambda$ states with masses of 4327 MeV and 4467 MeV, respectively, which might very well correspond with the recently observed $P_{\psi_s}^\Lambda(4338)$ [1] and the $P_{\psi_s}^\Lambda(4459)$ [2]. That is, the present model is compatible with most of the currently experimentally observed pentaquarks with the exception of the $P_{\psi}^N(4337)$ [27], the nature of which does not seem to fit within the molecular picture [28, 29]. Yet, caution is advised as it remains unclear

whether the $P_{\psi}^N(4457)$ and $P_{\psi_s}^{\Lambda}(4338)$ are actual molecules or not [8, 69, 70].

Besides the previous molecular pentaquarks, we predict a relatively rich spectrum of new, so far unobserved states. The eventual experimental observation (or absence) of these states will be able to confirm (or refute) the present phenomenological model, and thus indirectly constrain the nature of the currently known pentaquarks. It is also worth noticing that previous theoretical works have predicted molecular spectra that are similar to ours [15–19, 35, 51]. Even though the quantitative details of the spectrum might change by varying the parameters or by choosing a different input state (a point that we have partially explored for a few selected molecules by using the $P_{\psi}^{\Lambda}(4338)$ and $P_{\psi_s}^{\Lambda}(4459)$ as the reference state), there are two important qualitative characteristics of the predicted spectrum: everything else being equal, we have that

- (i) the central and spin-spin potentials of molecular hidden-charm pentaquarks tend to be more attractive if they are in the smaller-sized representations of SU(3)-flavor, i.e. singlets are more attractive than octets for $\bar{H}_c T_c$ configurations and, provided the evaluation of the spin-spin operator is positive (i.e. meson-baryon configurations with the maximum possible spin, $J = J_1 + J_2$), octets will also be more attractive than decuplets in $\bar{H}_c S_c$, and
- (ii) for the $\bar{H}_c S_c$ configurations, which contain non-trivial dependence on the light-spin of the heavy hadrons, higher spin states are lighter (heavier) for the octet (de-

cuplet) configurations.

For instance, as a consequence of (i) we expect the most attractive $\bar{H}_c T_c$ pentaquarks to be the isoscalar $\bar{D}^{(*)}\Xi_c$ configurations, which correspond with the molecular interpretation of the $P_{\psi_s}^{\Lambda}(4338/4459)$. Meanwhile, from (ii) if the $P_{\psi}^N(4440/4457)$ are $\bar{D}^*\Sigma_c$ bound states, then the $P_{\psi}^N(4440)$ should be $J = \frac{3}{2}$ and the $P_{\psi}^N(4457)$ $J = \frac{1}{2}$ (because higher spin implies lighter mass in the present model). The eventual experimental determination of the spin of the $P_{\psi}^N(4440)$ as well as the discovery of new pentaquarks (particularly decuplets) would indeed shed light on whether the previous patterns are correct.

ACKNOWLEDGMENTS

This work is partly supported by the National Natural Science Foundation of China under Grants No. 11735003, No. 11835015, No. 11975041, No. 12047503, No. 12125507 and No. 12305096, the Chinese Academy of Sciences under Grant No. XDB34030000, the Postdoctoral Fellowship Program of the China Postdoctoral Science Foundation under Grant Number GZC20241765, the Fundamental Research Funds for the Central Universities under Grant No. SWU-KQ25016 and the Thousand Talents Plan for Young Professionals. M.P.V. would also like to thank the IJCLab of Orsay, where part of this work has been done, for its long-term hospitality.

-
- [1] R. Aaij *et al.* (LHCb), Phys. Rev. Lett. **131**, 031901 (2023), arXiv:2210.10346 [hep-ex].
 - [2] R. Aaij *et al.* (LHCb), Sci. Bull. **66**, 1391 (2021), arXiv:2012.10380 [hep-ex].
 - [3] R. Aaij *et al.* (LHCb), Phys. Rev. Lett. **122**, 222001 (2019), arXiv:1904.03947 [hep-ex].
 - [4] M. Karliner and J. L. Rosner, Phys. Rev. D **106**, 036024 (2022), arXiv:2207.07581 [hep-ph].
 - [5] F.-L. Wang and X. Liu, Phys. Lett. B **835**, 137583 (2022), arXiv:2207.10493 [hep-ph].
 - [6] M.-J. Yan, F.-Z. Peng, M. Sánchez Sánchez, and M. Pavon Valderrama, Phys. Rev. D **107**, 074025 (2023), arXiv:2207.11144 [hep-ph].
 - [7] L. Meng, B. Wang, and S.-L. Zhu, Phys. Rev. D **107**, 014005 (2023), arXiv:2208.03883 [hep-ph].
 - [8] T. J. Burns and E. S. Swanson, Phys. Lett. B **838**, 137715 (2023), arXiv:2208.05106 [hep-ph].
 - [9] H.-X. Chen, W. Chen, X. Liu, and X.-H. Liu, Eur. Phys. J. C **81**, 409 (2021), arXiv:2011.01079 [hep-ph].
 - [10] F.-Z. Peng, M.-J. Yan, M. Sánchez Sánchez, and M. P. Valderrama, Eur. Phys. J. C **81**, 666 (2021), arXiv:2011.01915 [hep-ph].
 - [11] M.-Z. Liu, Y.-W. Pan, and L.-S. Geng, Phys. Rev. D **103**, 034003 (2021), arXiv:2011.07935 [hep-ph].
 - [12] R. Chen, Phys. Rev. D **103**, 054007 (2021), arXiv:2011.07214 [hep-ph].
 - [13] R. Chen, Z.-F. Sun, X. Liu, and S.-L. Zhu, Phys. Rev. D **100**, 011502 (2019), arXiv:1903.11013 [hep-ph].
 - [14] H.-X. Chen, W. Chen, and S.-L. Zhu, Phys. Rev. D **100**, 051501 (2019), arXiv:1903.11001 [hep-ph].
 - [15] M.-Z. Liu, Y.-W. Pan, F.-Z. Peng, M. Sánchez Sánchez, L.-S. Geng, A. Hosaka, and M. Pavon Valderrama, Phys. Rev. Lett. **122**, 242001 (2019), arXiv:1903.11560 [hep-ph].
 - [16] C. Xiao, J. Nieves, and E. Oset, Phys. Rev. D **100**, 014021 (2019), arXiv:1904.01296 [hep-ph].
 - [17] M. Pavon Valderrama, Phys. Rev. D **100**, 094028 (2019), arXiv:1907.05294 [hep-ph].
 - [18] M.-Z. Liu, T.-W. Wu, M. Sánchez Sánchez, M. P. Valderrama, L.-S. Geng, and J.-J. Xie, Phys. Rev. D **103**, 054004 (2021), arXiv:1907.06093 [hep-ph].
 - [19] F.-K. Guo, H.-J. Jing, U.-G. Meißner, and S. Sakai, Phys. Rev. D **99**, 091501 (2019), arXiv:1903.11503 [hep-ph].
 - [20] Y.-W. Pan, M.-Z. Liu, F.-Z. Peng, M. Sánchez Sánchez, L.-S. Geng, and M. Pavon Valderrama, Phys. Rev. D **102**, 011504 (2020), arXiv:1907.11220 [hep-ph].
 - [21] M. I. Eides, V. Y. Petrov, and M. V. Polyakov, Mod. Phys. Lett. A **35**, 2050151 (2020), arXiv:1904.11616 [hep-ph].
 - [22] F. Stancu, Phys. Rev. D **101**, 094007 (2020), arXiv:2004.06009 [hep-ph].
 - [23] J. Ferretti and E. Santopinto, JHEP **04**, 119 (2020), arXiv:2001.01067 [hep-ph].

- [24] J. Ferretti and E. Santopinto, *Sci. Bull.* **67**, 1209 (2022), arXiv:2111.08650 [hep-ph].
- [25] H. Garcilazo and A. Valcarce, *Phys. Rev. D* **105**, 114016 (2022), arXiv:2207.02757 [hep-ph].
- [26] P. G. Ortega, D. R. Entem, and F. Fernandez, *Phys. Lett. B* **838**, 137747 (2023), arXiv:2210.04465 [hep-ph].
- [27] R. Aaij *et al.* (LHCb), *Phys. Rev. Lett.* **128**, 062001 (2022), arXiv:2108.04720 [hep-ex].
- [28] M.-J. Yan, F.-Z. Peng, M. Sánchez Sánchez, and M. Pavon Valderrama, *Eur. Phys. J. C* **82**, 574 (2022), arXiv:2108.05306 [hep-ph].
- [29] S. X. Nakamura, A. Hosaka, and Y. Yamaguchi, *Phys. Rev. D* **104**, L091503 (2021), arXiv:2109.15235 [hep-ph].
- [30] F.-Z. Peng, M. Sánchez Sánchez, M.-J. Yan, and M. Pavon Valderrama, *Phys. Rev. D* **105**, 034028 (2022), arXiv:2101.07213 [hep-ph].
- [31] J.-J. Wu, R. Molina, E. Oset, and B. S. Zou, *Phys. Rev. C* **84**, 015202 (2011), arXiv:1011.2399 [nucl-th].
- [32] J.-J. Wu and B. S. Zou, *Phys. Lett. B* **709**, 70 (2012), arXiv:1011.5743 [hep-ph].
- [33] W. L. Wang, F. Huang, Z. Y. Zhang, and B. S. Zou, *Phys. Rev. C* **84**, 015203 (2011), arXiv:1101.0453 [nucl-th].
- [34] C. W. Xiao, J. Nieves, and E. Oset, *Phys. Rev. D* **88**, 056012 (2013), arXiv:1304.5368 [hep-ph].
- [35] C. W. Xiao, J. Nieves, and E. Oset, *Phys. Lett. B* **799**, 135051 (2019), arXiv:1906.09010 [hep-ph].
- [36] X.-K. Dong, F.-K. Guo, and B.-S. Zou, *Progr. Phys.* **41**, 65 (2021), arXiv:2101.01021 [hep-ph].
- [37] R. L. Workman *et al.* (Particle Data Group), *PTEP* **2022**, 083C01 (2022).
- [38] M. Gell-Mann and M. Levy, *Nuovo Cim.* **16**, 705 (1960).
- [39] D. O. Riska and G. E. Brown, *Nucl. Phys. A* **679**, 577 (2001), arXiv:nucl-th/0005049 [nucl-th].
- [40] J. J. Sakurai, *Annals Phys.* **11**, 1 (1960).
- [41] K. Kawarabayashi and M. Suzuki, *Phys. Rev. Lett.* **16**, 255 (1966).
- [42] Riazuddin and Fayyazuddin, *Phys. Rev.* **147**, 1071 (1966).
- [43] F.-Z. Peng, M.-Z. Liu, M. Sánchez Sánchez, and M. Pavon Valderrama, *Phys. Rev. D* **102**, 114020 (2020), arXiv:2004.05658 [hep-ph].
- [44] M. Pavón Valderrama and D. R. Phillips, *Phys. Rev. Lett.* **114**, 082502 (2015), arXiv:1407.0437 [nucl-th].
- [45] T. A. Kaeding, *Atom. Data Nucl. Data Tabl.* **61**, 233 (1995), arXiv:nucl-th/9502037 [nucl-th].
- [46] S. X. Nakamura and J. J. Wu, *Phys. Rev. D* **108**, L011501 (2023), arXiv:2208.11995 [hep-ph].
- [47] K. Chen, Z.-Y. Lin, and S.-L. Zhu, *Phys. Rev. D* **106**, 116017 (2022), arXiv:2211.05558 [hep-ph].
- [48] S. Adhikari *et al.* (GlueX), *Phys. Rev. C* **108**, 025201 (2023), arXiv:2304.03845 [nucl-ex].
- [49] I. Strakovsky, W. J. Briscoe, E. Chudakov, I. Larin, L. Pentchev, A. Schmidt, and R. L. Workman, *Phys. Rev. C* **108**, 015202 (2023), arXiv:2304.04924 [hep-ph].
- [50] Y. Yamaguchi, H. García-Tecocoatzi, A. Giachino, A. Hosaka, E. Santopinto, S. Takeuchi, and M. Takizawa, *Phys. Rev. D* **101**, 091502 (2020), arXiv:1907.04684 [hep-ph].
- [51] B. Wang, L. Meng, and S.-L. Zhu, *Phys. Rev. D* **101**, 034018 (2020), arXiv:1912.12592 [hep-ph].
- [52] M.-L. Du, V. Baru, F.-K. Guo, C. Hanhart, U.-G. Meißner, J. A. Oller, and Q. Wang, *Phys. Rev. Lett.* **124**, 072001 (2020), arXiv:1910.11846 [hep-ph].
- [53] F.-Z. Peng, M.-Z. Liu, Y.-W. Pan, M. Sánchez Sánchez, and M. Pavon Valderrama, *Nucl. Phys. B* **983**, 115936 (2022), arXiv:1907.05322 [hep-ph].
- [54] E. Santopinto and A. Giachino, *Phys. Rev. D* **96**, 014014 (2017), arXiv:1604.03769 [hep-ph].
- [55] M. I. Eides, V. Y. Petrov, and M. V. Polyakov, *Eur. Phys. J. C* **78**, 36 (2018), arXiv:1709.09523 [hep-ph].
- [56] R. Chen, X. Liu, X.-Q. Li, and S.-L. Zhu, *Phys. Rev. Lett.* **115**, 132002 (2015), arXiv:1507.03704 [hep-ph].
- [57] F.-L. Wang, X.-D. Yang, R. Chen, and X. Liu, *Phys. Rev. D* **103**, 054025 (2021), arXiv:2101.11200 [hep-ph].
- [58] T. J. Burns, *Eur. Phys. J. A* **51**, 152 (2015), arXiv:1509.02460 [hep-ph].
- [59] L. Geng, J. Lu, and M. P. Valderrama, *Phys. Rev. D* **97**, 094036 (2018), arXiv:1704.06123 [hep-ph].
- [60] T. J. Burns and E. S. Swanson, *Phys. Rev. D* **100**, 114033 (2019), arXiv:1908.03528 [hep-ph].
- [61] F.-Z. Peng, J.-X. Lu, M. Sánchez Sánchez, M.-J. Yan, and M. Pavon Valderrama, *Phys. Rev. D* **103**, 014023 (2021), arXiv:2007.01198 [hep-ph].
- [62] N. Yalikul, Y.-H. Lin, F.-K. Guo, Y. Kamiya, and B.-S. Zou, *Phys. Rev. D* **104**, 094039 (2021), arXiv:2109.03504 [hep-ph].
- [63] S. Sakai, H.-J. Jing, and F.-K. Guo, *Phys. Rev. D* **100**, 074007 (2019), arXiv:1907.03414 [hep-ph].
- [64] F.-Z. Peng, M.-J. Yan, M. S. Sánchez, and M. Pavon Valderrama, *Phys. Lett. B* **846**, 138207 (2023), arXiv:2211.09154 [hep-ph].
- [65] R. Aaij *et al.* (LHCb), *Phys. Rev. D* **110**, 032001 (2024), arXiv:2404.07131 [hep-ex].
- [66] M. Albaladejo, F.-K. Guo, C. Hidalgo-Duque, and J. Nieves, *Phys. Lett. B* **755**, 337 (2016), arXiv:1512.03638 [hep-ph].
- [67] C. Fernández-Ramírez, A. Pilloni, M. Albaladejo, A. Jackura, V. Mathieu, M. Mikhasenko, J. A. Silva-Castro, and A. P. Szczepaniak (JPAC), *Phys. Rev. Lett.* **123**, 092001 (2019), arXiv:1904.10021 [hep-ph].
- [68] Z. Yang, X. Cao, F.-K. Guo, J. Nieves, and M. P. Valderrama, *Phys. Rev. D* **103**, 074029 (2021), arXiv:2011.08725 [hep-ph].
- [69] S.-Q. Kuang, L.-Y. Dai, X.-W. Kang, and D.-L. Yao, *Eur. Phys. J. C* **80**, 433 (2020), arXiv:2002.11959 [hep-ph].
- [70] T. J. Burns and E. S. Swanson, *Eur. Phys. J. A* **58**, 68 (2022), arXiv:2112.11527 [hep-ph].